

**PERFORMANCE EVALUATION OF TURBO-CODED
MC-CDMA OVER BROADBAND POWERLINE CHANNEL**

A DISSERTATION

*Submitted in partial fulfillment of the
requirements for the award of the degree*

of

MASTER OF TECHNOLOGY

in

ELECTRONICS & COMMUNICATION ENGINEERING

(With Specialization in Communication Systems)

By

AMIT KUMAR BANSAL



DEPARTMENT OF ELECTRONICS & COMPUTER ENGINEERING

INDIAN INSTITUTE OF TECHNOLOGY ROORKEE

ROORKEE - 247 667 (INDIA)

JUNE 2007

CANDIDATE'S DECLARATION

I hereby declare that the work, which is presented in this dissertation entitled **"PERFORMANCE EVALUATION OF TURBO-CODED MC-CDMA OVER BROADBAND POWERLINE CHANNEL"** submitted in partial fulfillment of the requirements for the award of the degree of **Master of Technology in Electronics and Communication Engineering** with specialization in **Communication Systems**, in the Department of Electronics and Computer Engineering, Indian Institute of Technology, Roorkee, is an authentic record of my own work carried out from July 2006 to June 2007, under the guidance and supervision of **Mr. S. CHAKRAVORTY**, Assistant Professor, Department of Electronics and Computer Engineering, Indian Institute of Technology, Roorkee.

The results embodied in this dissertation have not been submitted for the award of any other Degree or Diploma.

Date: 29-06-2007

Place: Roorkee

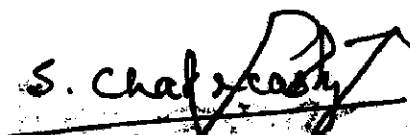

AMIT KUMAR BANSAL

CERTIFICATE

This is to certify that the statement made by the candidate is correct to the best of my knowledge and belief.

Date: 29-06-2007

Place: Roorkee


Mr. S. CHAKRAVORTY
Assistant Professor, E&CE Department,
Indian Institute of Technology Roorkee
Roorkee - 247 667, (INDIA)

ACKNOWLEDGEMENT

It is my privilege and pleasure to express my profound sense of respect, gratitude and indebtedness to my guide, **Mr. S. Chakravorty**, Professor, Department of Electronics and Computer Engineering, Indian Institute of Technology, Roorkee, for his inspiration, guidance, constructive criticisms and encouragement throughout this dissertation work.

I express my sincere thanks to **Dr D. K. Mehra**, Professor and Head, Department of Electronics and Computer Engineering, Indian Institute of Technology, Roorkee, for providing necessary facilities and morale support throughout this dissertation work.

Next, I feel indebted to all those endless researchers all over the world whose work I have used for my dissertation work. Their sincerity and devotion motivates me most. Thanks are due to the Lab staff of Communication Systems Lab, Department of Electronics and Computer Engineering, Indian Institute of Technology, Roorkee, for their cooperation.

I am greatly indebted to all my friends, who have graciously applied themselves to the task of helping me with ample morale support and valuable suggestions. Most of all, I would like to thank my family. My parents provided me a perfect environment for my studies and supported me throughout.

Finally, I would like to extend my gratitude to all those persons who directly or indirectly helped me in the process and contributed towards this work.

AMIT KUMAR BANSAL

ABSTRACT

In recent years, the use of existing power lines for transmitting data and voice has been receiving interest. The main advantages of power line communications (PLC) is the ubiquity of power lines and power outlets. Now a days, PLC is emerging as a new technology for broadband services such as fast Internet access, telephone and fax services, and home networking. The severity of noise, attenuation and multipath propagation pose challenges for communications over power lines. Impulsive noise and multipath effects are the main reasons that cause burst errors in power line communications. To nullify these effects, robust modulation and coding schemes are needed.

In this dissertation, the BER performance of Turbo codes combined with MC-CDMA is evaluated for the broadband powerline (BPL) channel environment with different combining techniques. The performance is evaluated for single user and multi-user case. For simulating the channel, multipath model proposed by Zimmermann and Dostert is used. This model is based on physical signal propagation effects in mains networks including numerous branches and impedance mismatching. Impulsive noise in the channel has been modeled using Middleton's class A noise model. The performance of Turbo coded MC-CDMA system is compared with uncoded MC-CDMA system and significant coding gain is achieved as shown by simulation results. A performance comparison of Turbo-coded MC-CDMA is also done with other available coding techniques in the broadband powerline channel environment.

CONTENTS

	Page
CANDIDATE'S DECLARATION	i
CERTIFICATE	i
ACKNOWLEDGEMENT	ii
ABSTRACT	iii
CHAPTER 1: INTRODUCTION	1
1.1 The Powerline Channel as a Transmission Medium.....	2
1.2 Coding and Modulation Techniques for PLC.....	3
1.3 Statement of the Problem.....	5
1.4 Organization of the Report.....	6
CHAPTER 2: POWER LINE CHANNEL	7
2.1 Broadband PLC Channel Characterization.....	8
2.2 Channel Models.....	9
2.2.1 Analytical Model.....	10
2.2.2 Measurement based Model.....	10
2.2.3 Models based on MTL Theory.....	12
2.2.4 Other Channel Models.....	13
2.3 Noise.....	16
2.3.1 Impulsive Noise Model.....	18
2.3.2 Simplified Class A Noise Model.....	19
CHAPTER 3: MC-CDMA OVER BROADBAND POWERLINE CHANNEL	21
3.1 Uncoded MC-CDMA over Broadband Powerline Channel.....	22
3.1.1 MC-CDMA Transmitter.....	24
3.1.2 MC-CDMA Receiver.....	25

3.1.3	Combining Techniques.....	26
3.2	Coded MC CDMA over Broadband Powerline Channel.....	28
3.2.1	Turbo Encoder.....	28
3.2.2	Turbo Decoder.....	31
3.2.2.1	Iterative MAP Algorithm.....	32
3.2.2.2	Algorithm steps of Iterative MAP Decoding Method.....	34
3.3	Performance of Uncoded and Coded MC CDMA over BPL.....	35
 CHAPTER 4: SIMULATION		 38
4.1	System Model.....	38
4.2	Powerline Channel.....	39
4.3	Impulsive Noise.....	40
4.4	System parameters for the Coded MC CDMA.....	42
 CHAPTER 5: RESULTS AND DISCUSSION		 48
5.1	Channel Model.....	48
5.2	Impulsive Noise Model.....	50
5.3	Performance of Turbo coding in Impulsive Noise Environment.....	50
5.4	Performance of MC-CDMA over BPL with Impulsive Noise.....	52
5.5	Performance of Turbo coded MC-CDMA over BPL with Impulsive Noise.....	55
5.6	Performance Comparison of Turbo coded MC-CDMA with other Coding Techniques.....	58
 CHAPTER 6: CONCLUSION		 59
6.1	Scope for Future Work.....	59
 REFERENCES		 61
 APPENDIX: MATLAB CODE		 64

CHAPTER 1

INTRODUCTION

Digital communications over power lines is not a new idea, as several power utility companies have used power line communications (PLCs) for a couple of decades for narrowband applications such as metering and control. In the past few years, however, there has been a renewed interest in the possibility of exploiting power line cables as a *broadband* communications medium. Moreover, as opposed to the past, today's interest spans several important applications: broadband Internet access, indoor wired local area network (LAN) for residential and business premises, in-vehicle data communications, smart grid applications (advanced metering and control, peak shaving, mains monitoring), and other municipal applications, such as traffic lights and lighting control, security, etc.

The basic rationale for such enthusiasm is that the power grid provides an infrastructure that is much more extensive and pervasive than any other wired alternative, and that virtually every line-powered device can become the target of value added services. Therefore, PLCs may be considered as the technological enabler of a plethora of future applications that would probably not be available otherwise. Despite all this recent enthusiasm, there is still some skepticism about the technology and its commercial viability. This skepticism is due to technical challenges, regulatory issues, and to the fact that today there is still no available standard [1]. The main technical challenges of PLCs are: the power line channel is a very harsh and noisy transmission medium that is very difficult to model; the power line channel is frequency-selective, time-varying, and is impaired by colored background noise and impulsive noise; many transformers along the power line are fed by a single high-voltage line, with the earth itself being used for the return electrical path (a very noisy configuration for telecommunications signals); the structure of the grid differs from country to country and also within a country, and the same applies for indoor wiring practices; power line cables are often unshielded, thus becoming both sources and targets of electromagnetic interference (EMI); last but not

least, regulations about electromagnetic compatibility (EMC) differ on a country-by-country basis [2].

1.1 The Powerline Channel as a Transmission Medium

Power lines constitute a rather hostile medium for data transmission. Varying impedance, considerable noise, and high attenuation are the main issues. The channel mixes the nasty behavior of a power line with that of a communication channel. The channel between any two outlets in a home has the transfer function of an extremely complicated line network. Many stubs have transmission loads of various impedances. Over such a transmission medium, the amplitude and phase response may vary widely with frequency. While the signal may arrive at the receiver with very little loss over some frequencies, it may be completely indistinguishable over other frequencies. Worse, the channel transfer function itself is time varying since plugging in or switching off of devices connected to the network would change the network topology.

The location of the transmitter or the receiver (in this case the power outlet) could also have a serious effect on transmission error rates. For example, a receiver close to a noise source would have a poor signal to noise ratio (SNR) compared to one further away from the noise source. The noise sources could be home devices plugged into the network. Just like a wireless channel, signal propagation does not take place between the transmitter and the receiver along a line-of-sight path. As a result, additional echoes must be considered. This echoing occurs because a number of propagation paths exist between the transmitter and the receiver. Reflection of the signal often occurs due to the various impedance mismatches in the electric network. Each multi-path would have a certain weight factor attributed to it to account for the reflection and transmission losses. All reflection and transmission parameters in a power line channel may be assumed to be less than one. The number of dominant multi-paths to be considered (N) is often not more than five or six since additional multi-paths are usually too weak to be of any significance. This is because the more transitions and reflections that occur along a path, the smaller its weighting factor would be. It has been observed from channel measurements that at higher frequencies the channel attenuation increases [3]. Hence, the

channel may be described as random and time varying with a frequency dependent signal to noise ratio (SNR) over the transmission bandwidth.

Another significant problem in power lines is noise. This is because it rarely has properties similar to the easily analyzed white Gaussian noise of the receiver front ends. Typical sources of noise are brush motors, fluorescent and halogen lamps, switching power supplies and dimmer switches. The noise in power lines can be impulsive or frequency selective in nature and sometimes both [4].

1.2 Coding and Modulation Techniques for PLC

The ultimate capability of a channel in terms of data rate can be evaluated by computing its capacity, which also yields guidelines on the most appropriate coding schemes to be applied. For PLC, the situation is complicated by the fact that a general channel model has not been agreed upon; hence robust modulation and channel coding techniques are required.

For narrowband applications on power lines, single-carrier modulation has been adopted for its simplicity, employing frequency shift keying (FSK), quadrature phase shift keying (QPSK), or other modulation method [5]. However, in broadband applications on power line channels, these techniques have been shown to be inadequate for high-speed communications. The principal problem is frequency-selective fading, which places deep notches in the frequency response, whose locations vary from cable to cable, time to time, and location to location. If the signaling band contains such an unfavorable notch, very poor system performance can be expected. Another problem arises when trying to use the rest of the spectrum: usually the channel attenuation increases with frequency, and many bands are not flat enough to accommodate high rate communications with narrowband modulation. Also, the signal is easy to localize in frequency and to disturb deliberately. Similar considerations in wireless and DSL communications have given rise to two powerful techniques for combating multi-path fading and inter-symbol interference (ISI): spread spectrum and multi-carrier modulation (MCM).

As a wideband modulation approach, spread spectrum techniques can exploit spectral diversity (e.g., through a RAKE receiver for direct sequence spread spectrum) to effectively combat multi-path fading, resulting in its wide spread use in mobile radio communications. Furthermore, spread spectrum is well known for its ability to suppress the effects of narrowband and other types of interference. Of course, spread spectrum comes in several varieties: direct sequence, frequency hopping, time hopping, chirp, and hybrid methods. The direct sequence (DS) spread spectrum techniques have the ability to realize a multiple access structure in a simple way by choosing suitable spreading sequences, that is, code-division multiple access (CDMA), and hence is widely used in practical communication systems.

MCM, achieves the highest performance in channels with frequency-selective fading and severe ISI [6]. The underlying rationale of MCM is to divide and conquer: a channel is divided into many independent ISI-free sub channels in the frequency domain, and power and bits are allocated adaptively according to the channel characteristics. The advantages of using MCM for communications over frequency-selective fading and ISI channels include optimality for data transmission, adaptivity to changing environments, and flexibility in bandwidth management. Furthermore, the demodulation and modulation processes have very low complexity when the fast Fourier Transform (FFT) and its inverse, IFFT, are used: There are many different names for this technique. In DSL applications it is often called discrete multi-tone (DMT), while in wireless applications it is better known as orthogonal frequency-division multiplexing (OFDM).

Generally the performance of MCM systems is limited by the sub-channels with the worst SNRs in a frequency-selective fading channel, and adaptive bit loading and power allocation is almost a necessity for efficient MCM transmission in practice. However, this adaptation is a complication in the transmission protocol and is sometimes not even appropriate (as in point-to-multipoint broadcast applications or time-varying mobile channels). The common approach to MCM over unknown channels is to use the same allocation to all frequencies and use advanced signal processing to improve the

performance at the frequencies that are found to be attenuated at the receiver. MCM is also robust to narrowband interference and impulse noise.

Multi-carrier Code Division Multiple Access is a combination of CDMA and OFDM. MC-CDMA not only has inherent narrowband interference suppression characteristic, but also an impulse noise effects mitigation capability [4]. In Multi-carrier CDMA there are three different forms. They are Multi-carrier (MC-CDMA), Multi-carrier DS-SS-CDMA and Multi-Tone (MT-SS-CDMA). Advantage of MC-CDMA over OFDM is that it can lower the symbol rate in each sub-carrier so that longer duration makes it easier to quasi-synchronize the transmissions. Short duration and high magnitude impulsive noise in powerline channel limit the performance in high speed data transmission applications. Impulsive noise is typically combated with forward error correction (FEC). To enable the correction of long burst of errors interleaving can be used to spread the burst over many code words. In this dissertation work Turbo codes are used as FEC codes, whose performance in terms of Bit Error Rate (BER) is close to the Shannon limit [7].

1.3 Statement of the Problem

For high speed communications, power lines present a hostile medium containing frequency selective fading, time varying behavior and highly disturbing noisy environment. The hostile noise environment present in power line has a spectrum containing background AWGN and a combination of impulsive noises. Since impulsive noise can cause burst errors, forward error correction strategies are must. To utilize powerlines for internet access and as a solution to last-mile problem require a robust modulation techniques such as MC-CDMA, OFDM. The main objectives in this work are:

- a) To study the Channel models and impulsive noise models for the powerline communication
- b) To study the performance of MC CDMA with different combining techniques over broadband powerline channel
- c) To study the performance of Turbo coding combined with MC CDMA over broadband powerline channel

1.4 Organization of the Report

This report is organized in six chapters. *Chapter 1* is introductory chapter and includes some basic concepts about powerline communications, its advantages, challenges and other relevant issues. *Chapter 2* contains the discussion of the different channel and impulsive noise models for broadband powerline communications and properties of powerline channel. *Chapter 3* explores the concepts of MC-CDMA which is used as the modulation technique for combating multi-path and fading characteristics of the powerline channel. MC CDMA utilizes the power of spread spectrum and OFDM both. Coded and uncoded MC-CDMA both are discussed. *Chapter 4* presents the step by step approach for simulation along with simulation parameter and simulation environment. *Chapter 5* contains the results and discussion of the results. *Chapter 6* includes the concluding remarks and scope for future work

CHAPTER 2

POWER LINE CHANNEL

Power line carrier was not specifically designed for data transmission and provides a harsh environment for it. Varying impedance, considerable noise that is not white in nature and high levels of frequency-dependent attenuation are the main issues. PLC channels (Fig. 2.1) suffer from a number of technical problems [5]:

- Frequency-varying and time-varying attenuation of the medium
- Dependence of the channel model on location, network topology, and connected loads
- High interference due to noisy loads
- High, nonwhite background noise
- Various forms of impulse noise
- Electromagnetic compatibility (EMC) issues that limit available transmitted power

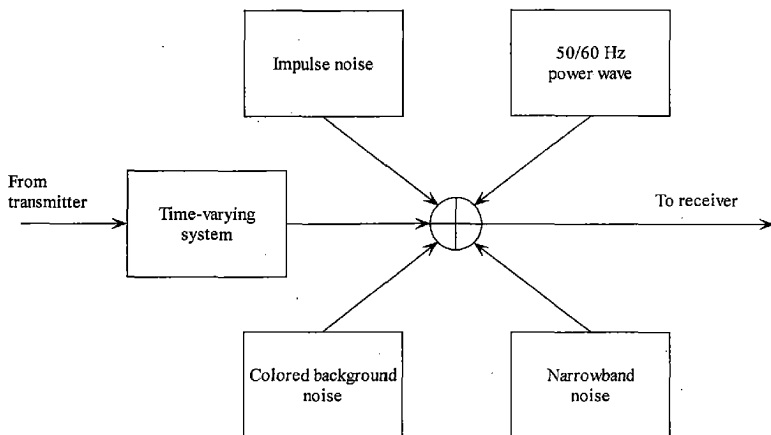


Figure 2.1 Block Diagram of a PLC channel [5]

2.1 Broadband PLC Channel Characterization

Due to the non-ideality of the conductors and insulation materials, part of the power that the transmitter injects into the cable does not reach the receiver, hence signal attenuates. Attenuation for two typical indoor PLC channels is shown in Figure 2.2 [8]. The PLC channels are far from ideal. The deepest frequency notch reaches up to -27 dB. On the average, -10.1 to -14.2 dB degradation is observed over the 100 MHz bandwidth [8].

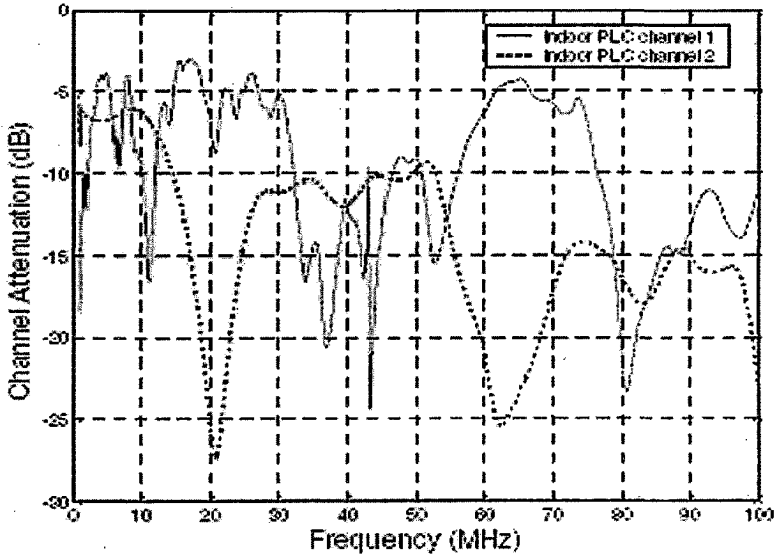
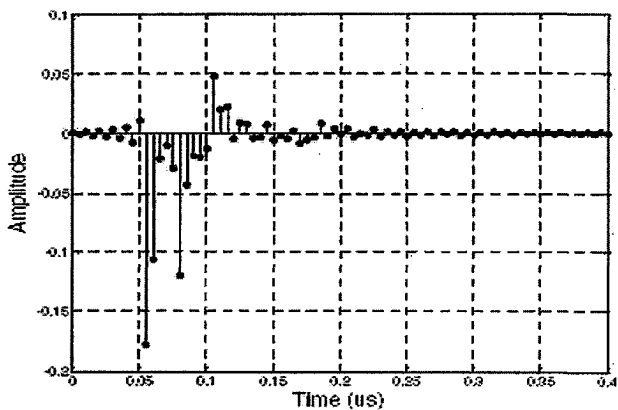
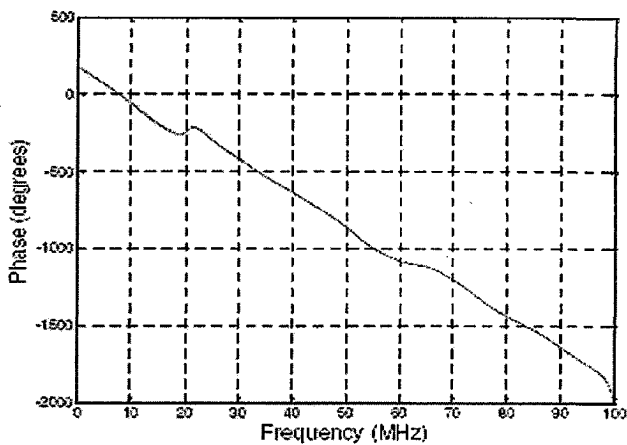


Figure 2.2 Different indoor PLC channels [8]

Taking the channel 2 as an example, Figure 2.3 [8] presents its impulse response and phase response. The channel owns time varying characteristics also due to the various devices that are plugged in/out and switched on/off in the powerline network. Furthermore, signals do not propagate along a single path, but suffer from reflections caused by impedance mismatches. Hence, the PLC channel can be regarded as a multipath environment with frequency-selective attenuation.



(a) Impulse response



(b) Phase response

Figure 2.3 An indoor PLC channel [8]

2.2 Channel Models

The powerline network differs considerably in topology, structure, and physical properties from conventional media such as twisted pair, coaxial, or fiber-optic cables.

PLC systems have to encounter rather hostile properties [5]. For computer simulations oriented to appropriate system design, models of the transfer characteristics of the mains network are of major interest. There are various channel models available for powerline channel in the literature [9] - [16]:

2.2.1 Analytical Model

Probably the most widely known model for the transfer function $H(f)$ of the PLC channel is the multipath model proposed by Zimmermann and Dostert [9], this is an analytic model describing complex transfer functions of typical powerline networks using only a small set of parameters. The model is based on physical signal propagation effects in mains networks including numerous branches and impedance mismatching. Besides multipath propagation accompanied by frequency selective fading, signal attenuation of typical power cables increasing with length and frequency is considered. The model takes the following form for $H(f)$ in the frequency range from 500 kHz to 20 MHz:

$$H(f) = \sum_{i=1}^N g_i \exp(-(a_0 + a_l f^k) d_i) \exp(-j2\pi f \tau_i) \quad \dots\dots(2.1)$$

Here N is the number of relevant propagation paths, a_0 and a_l are link attenuation parameters, k is an exponent (with typical values ranging from 0.5 to 1), g_i is the weighting factor for path i , d_i its length, and τ_i its delay.

The amplitude response, phase details and impulse response of a 15 path model are shown in fig. 2.4 [9]. Due to the reduced number of paths, the frequency response of model and measurement exhibit some differences above 4 MHz, especially at the locations of the deep notches. However, the impulse response is still covered quite well by the model.

2.2.2 Measurement based Model

Olaf G. Hooijen [10] proposed a channel model for the residential power circuit used as a carrier for telecommunications signals. This model is based on measurements. As a basis for the channel model, the time-variant linear filter model is used. Signal attenuation on the channel was shown to be a summation of coupling losses and line losses, both of

which can be very high, making it very difficult to transmit over distances of more than 500 m. It is also shown that the residential power circuit exhibits a phase shift that is virtually time invariant, indicating that phase-modulation techniques can probably be used successfully for communications over PLC. Effect of noise is also considered and background noise model in frequency range 9-95 kHz is presented [10]. The additive noise on the channel was shown to be a collection of four noise types:

- a) Spectrally flat noise with a power-spectral density that decreases for increasing frequency
- b) Impulse noise
- c) Noise at fixed frequencies correlated with the power system frequency
- d) Noise at fixed frequencies uncorrelated with the power system frequency

A distribution of the noise spectra is shown in figure 2.5 [10].

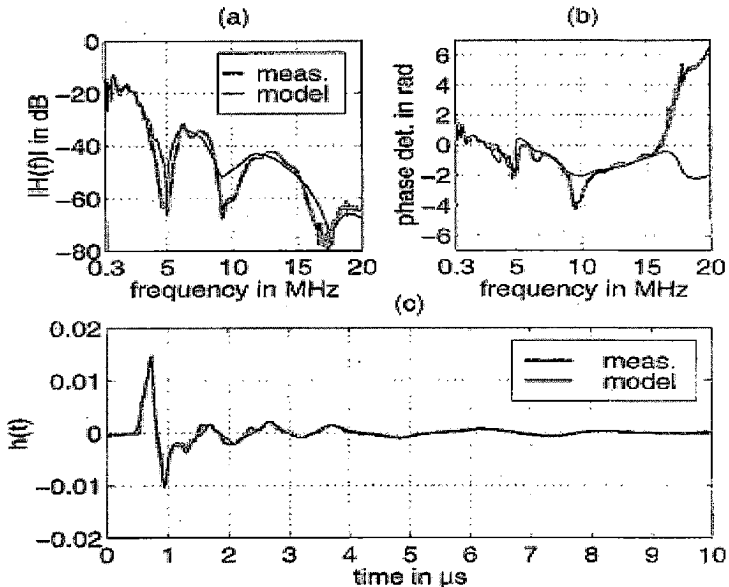


Figure 2.4 Reference model with 15 paths: (a) amplitude response, (b) phase details, and (c) impulse response [9]

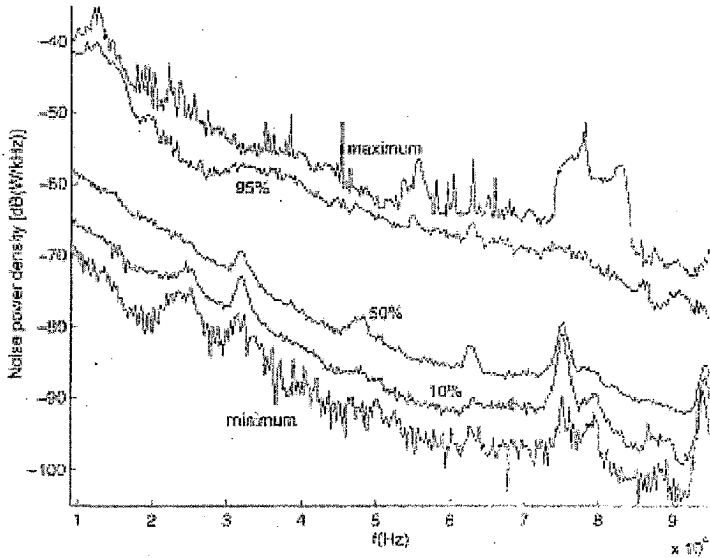


Figure 2.5 Distribution of the noise spectra measured in a rural environment [10]

2.2.3 Models based on MTL Theory

Stefano Galli, and Thomas C. Banwell [11] proposed the channel model based on Multi-conductor transmission line (MTL) theory. In this, authors [11] present analysis and data that validate the accuracy of the MTL approach and further justify its use in the PL channel context. It is also described in detail, the methodology to follow for modeling both grounded and ungrounded PL links in a unified framework. A consequence of the validity of the proposed modeling is that it can facilitate the process of standardization of the PL transfer function, an important step toward the availability of a commonly agreed upon (set of) channel transfer functions.

T. Sartenaer, and P. Delogne [12] proposed model for the deterministic modeling of the channel transfer functions associated with underground power line access networks, in the light of the Multi-conductor Transmission Line Theory. Multidimensional scattering matrix formalism is then introduced to perform an accurate analysis of the global power

line network including multi-conductor cable segments, derivation points, and termination loads.

2.2.4 Other Channel Models

Sami Barmada, Antonino Musolino, and Marco Raugi [13] proposed a wavelet based time domain model for the broadband characterization of power lines in presence of time variation of the loads. This model is characterized by taking into account both measured and geometrical channel characteristics and can be used to take into account the presence of noise. The channel is described by a two-port equivalent described by a scattering matrix determined from a wavelet-based expansion of the input and output quantities. Upper and lower bounds for the response of the channel in presence of time-varying loads are also determined [13]. The bound determination allows the estimate of noteworthy quantities for the tuning of currently used modulation schemes for power lines communications such as orthogonal frequency-division multiplexing. Considering the real situation, authors in [13] showed the performance of the proposed technique (shown in fig 2.6 to fig 2.8).

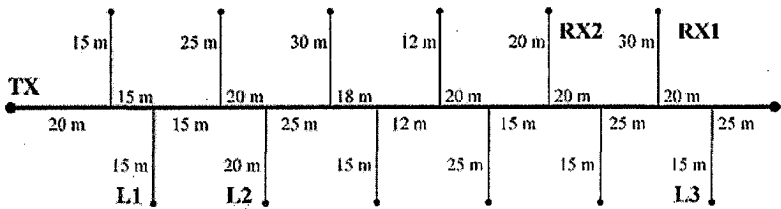


Figure 2.6 Realistic outdoor power line channel [13]

In fig.2.6, the labels have the following meanings: TX is the PLC transmitter, RX1 and RX2 are PLC receivers, L1, L2, and L3 are time-varying loads, the variation of the load impedance is assumed between the matched impedance value and the open circuit. In this case, the system has been excited by a pulse, characterized by a flat spectrum in the band 0.5–30 MHz where the frequency dependence of the cable parameters has been measured. The signal duration is about 0.2 s.

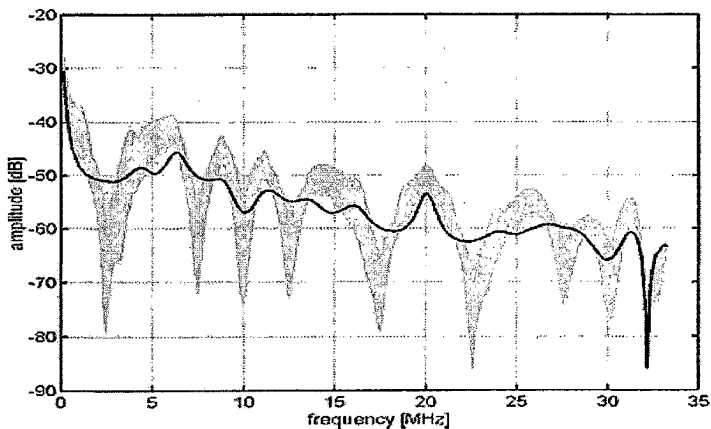


Figure 2.7 frequency characterization of the PLC channel for RX1. The grey curves are obtained when the not labeled terminations are all matched and L1, L2, and L3 vary between the matched impedance value and the open circuit. The bold line is obtained when all the terminations including L1, L2, and L3 are matched [13].

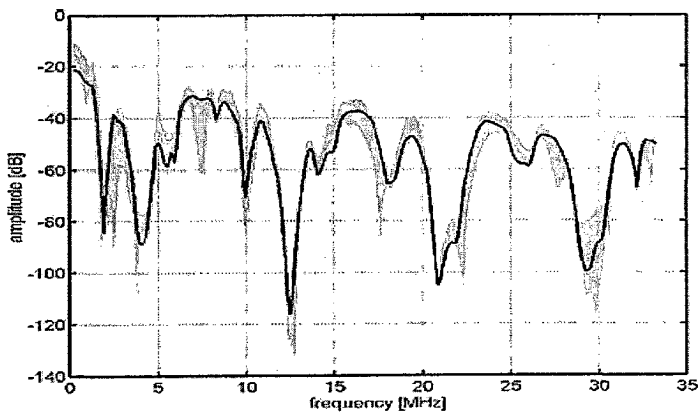


Figure 2.8 frequency characterization of the PLC channel for RX1. The grey curves are obtained when the not labeled termination are all open circuits and L1, L2, and L3 vary between the matched impedance value and the open circuit. The bold line is obtained when the terminations L1, L2, and L3 are matched [13].

The comparison of Figs.2.7 and 2.8 shows the major influence of the load variation on the channel response in the first case because the labeled impedance variations are evidenced by the matched configuration on the other ports. In the second case, the presence of open circuits on the not labeled terminations already heavily affects the channel response hiding the effects of the other terminations.

P. Karols, K. Dostert, G. Griepentrog, and S. Huettinger [14] presented channel model for special applications such as train automation in local transportation and mass transit (MT) systems. These DC-powered traction networks can be used as communication links between wayside equipment and the moving trains. As MT networks significantly differ from usual electricity supply systems, the usage of other common models and communication equipment for conventional PLC channels turns out infeasible. Authors [14] focus on MT channel investigation and modeling, in order to develop novel adapted solutions. The outcome is a stochastic MT channel model, which besides multipath and time-variance also includes peculiar properties such as the behavior of ring structures and the impact of the Doppler effect invoked by moving trains. In addition, a very special interference scenario is treated, caused by the rectifiers in these DC-powered environments.

C. J. Hatziaodoni, N. B. Harp, and A. J. Sugg [15] describe the application of finite elements for the modeling and simulation of overhead power-line structures in the high-frequency range, using existing computing tools and software. Authors [15] treat specifically non-uniform wire arrangements common in overhead power networks, including line junctions, bends, neutral grounding, etc., which disturb the transmission of signals, especially at high frequencies, increasing reflections, radiation, and mode conversion. The proposed [15] models could be used in applications associated with broadband communication over power lines providing a reliable representation for assessing the capability of the overhead network to carry high-frequency signals and estimate the resulting electromagnetic emissions. The efficacy of the proposed FE method for describing complex open-air line arrangements at frequencies above 30 MHz should be considered carefully.

Zheng Tao, Yang Xiaoxian, Zhang Baohui [16] analyze the physical signal propagation property with transmission theory, mode propagation theory and electromagnetic- field radiation theory. The conclusions of transmission characteristic by practical measurements and based on the analysis [16] are:

- The propagation signals are affected by attenuation increasing with frequency and length.
- The path loss is greatly dependent on the branches connected to the propagation path but has little correlation to the loads. Therefore, we may not pay much attention to the impact of load variations from the end users, which can reduce the complexity of the research.
- The signal propagation has more correlation to the network structure between the Tx and Rx, but the other parts of the power network have little impact on the signal propagation.
- The carrier signal radiation causes extra power loss dissipating into the space, which represents the integral effects of the power-line channel and spatial channel.

2.3 Noise

Unlike the other telecommunications channels, the noise characteristics in powerline environment cannot not be represented as an Additive White Gaussian Noise (AWGN), whose power spectral density is constant over the whole transmission spectrum. A lot of investigations and measurements were done in order to give a detailed description of the noise characteristics in a PLC environment. PLC noise can be classified as a superposition of five noise types, distinguished by their origin, time duration, spectrum occupancy and intensity [17]; the approximative representation of spectrum occupation is illustrated in Fig. 2.9. The various types of noise can be classified as follows:

- **Colored background noise (type 1)** this presents relatively low power spectral density (PSD), varying with frequency (its average value decreases as the frequency increases) and consisting mainly of a sum of numerous low-power noise sources. It is location dependent. The PSD is time variant from minutes up to hours.

- **Narrowband noise (type 2)**, this consists of continuous wave signals with amplitude modulation. This type of noise is produced mainly by ingress of broadcast stations operating in the medium and shortwave bands. Levels vary with the time of day.

- **Periodic impulsive noise, asynchronous to the main frequency (type 3)**, this noise is a form of impulses that usually has a repetition rate between 50 and 200 kHz, and which results in the spectrum with discrete lines with frequency spacing according to the repetition rate. This type of noise is mostly caused by switching power supplies. Because of its high repetition rate, this noise occupies frequencies that are too close to each other, and builds therefore frequency bundles that are usually approximated by narrow bands.

- **Periodic impulsive noise, synchronous to the main frequency (type 4)**, is impulses with a repetition rate of 50 or 100 Hz and are synchronous with the main powerline frequency. Such impulses have a short duration, in the order of microseconds, and have a power spectral density that decreases with the frequency. This type of noise is generally caused by power supply operating synchronously with the main frequency, such as the power converters connected to the mains supply.

- **Asynchronous impulsive noise (type 5)**, these impulses are rare single events, produced by on and off switching events. Impulse duration ranges from several microseconds to a few milliseconds with arbitrary arrival times. The PSD can be more than 60 dB above the background noise level.

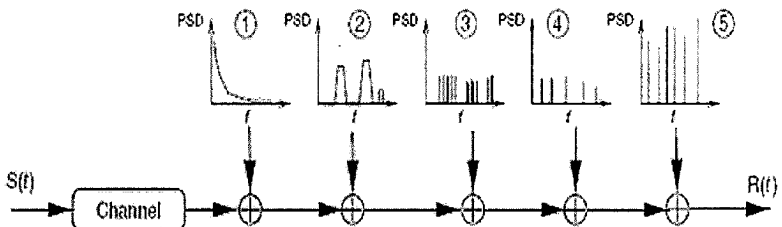


Figure 2.9 The additive noise types in PLC environments [18]

The approximate representation of spectrum occupation of the noise is illustrated in Fig. 2.9. The properties of noise types 1, 2 and 3 remain usually stationary over periods, of seconds, minutes and sometimes even of some hours, and may be summarized as “Generalized background noise” (fig 2.10).

The noise types 4 and 5 are, on the contrary, varying in time span of milliseconds and microseconds, and can be gathered in one noise class called as “impulse noise”. Because of its relatively higher amplitudes, impulse noise is considered the main cause of burst error occurrence in data transmitted over the high frequencies of the PLC medium. This can be modeled as a pulse train with pulse width t_w , pulse amplitude A , arrival time $t_{a,i}$ and a generalized pulse function $p(t/t_w)$ with unit amplitude and impulse width t_w (fig 2.11) [18].

$$n_{\text{imp}}(t) = \sum_{i=-\infty}^{\infty} A_i \cdot p\left(\frac{t - t_{a,i}}{t_{w,i}}\right)$$

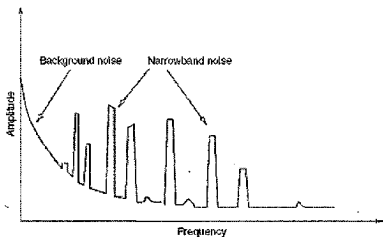


Figure 2.10 Spectral density model for the generalized background noise [18]

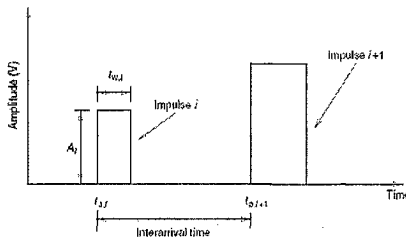


Figure 2.11 The impulse model used for impulsive noise class modeling [18]

2.3.1 Impulsive Noise Model

There are many noise models available proposed by different authors. One efficient method for the modeling of burst events is the use of Markov models; M. Zimmermann and K. Dostert, used a partitioned Markov chain, with a variable number of states per partition for modeling the impulsive noise [17]. Another popular model (proposed by D. Middleton) for impulsive noise environments is Middleton’s Class A noise model [19].

Middleton's Class A noise model can be used to model the impulsive interference in power line channels [19]. The probability density function (PDF) of Class A noise is given by

$$P_{A,\Gamma,\sigma^2}(z) = \sum_{m=0}^{\infty} \frac{e^{-A} A^m}{m!} \frac{1}{\sqrt{2\Gamma\sigma_m}} \exp\left(-\frac{z^2}{2\sigma_m^2}\right) \quad \dots\dots\dots (2.2)$$

$$\text{with } \sigma_m^2 = \sigma^2 \frac{m/A + \Gamma}{1 + \Gamma}$$

σ^2 is the total variance of the Class A noise, which is the sum of the variance of the Gaussian noise component σ_G^2 and impulsive noise component σ_I^2 ($\sigma^2 = \sigma_G^2 + \sigma_I^2$). Parameter A is the impulsive index which is defined as the product of the average number of impulses reaching the receiver in the time unit and the mean duration of the impulses. For small A (e.g. A= 0.1), we get highly structured (impulsive) noise where as for large values of A (above 10) the noise becomes Gaussian [19]. The parameter $\Gamma = (\sigma_G^2 / \sigma_I^2)$ is the Gauss-to-impulsive noise power ratio (GIR). Sources of impulsive noise are distributed with Poisson distribution $(e^{-A} A^m) / m!$. If one impulsive noise source generates a noise, then the noise is characterized by the Gaussian PDF with variance σ_I^2 / A . Consequently, at a certain observation time, assuming that the number of impulsive noise sources is m which is characterized by Poisson distribution with mean A, the noise of the receiver is characterized by the Gaussian PDF with variance $\sigma_m^2 = \sigma_G^2 + (m\sigma_I^2 / A)$.

2.3.2 Simplified Class A Noise Model

As the PDF of Class A noise consists of infinite series, it is intractable to develop receivers optimized in Class A noise [19]. If impulsive index A is smaller than 0.25, Eq. (2.2) is approximate to the sum of three terms in $m = 0, 1, 2$,

$$\hat{P}_{A,\Gamma,\sigma^2}(z) = \frac{e^{-A}}{\sqrt{2\Gamma\sigma^2}} \left(\frac{1}{\sigma_0} e^{-z^2/2\sigma_0^2} + \frac{A}{\sigma_1} e^{-z^2/2\sigma_1^2} + \frac{A^2}{2\sigma_2} e^{-z^2/2\sigma_2^2} - \frac{z^2}{2\sigma_m^2} \right) \dots(2.3)$$

with $\sigma_0^2 = \sigma^2 \frac{\Gamma}{1+\Gamma}$, $\sigma_1^2 = \sigma^2 \frac{1/A + \Gamma}{1+\Gamma}$, $\sigma_2^2 = \sigma^2 \frac{2/A + \Gamma}{1+\Gamma}$

Further, Eq. (2.3) can be approximate to

$$\hat{P}_{A,\Gamma,\sigma^2}(z) = \max_{m=0,1,2} \left[\frac{e^{-A} A^m}{m!} \frac{1}{\sqrt{2\Pi\sigma_m}} \exp\left(-\frac{z^2}{2\sigma_m^2}\right) \right]$$

$$= \begin{cases} e^{-A} \frac{1}{\sqrt{2\Pi\sigma_0}} \exp\left(-\frac{z^2}{2\sigma_0^2}\right), & 0 \leq |z| < a, \\ e^{-A} \frac{1}{\sqrt{2\Pi\sigma_1}} \exp\left(-\frac{z^2}{2\sigma_1^2}\right), & a \leq |z| < b, \\ e^{-A} \frac{1}{\sqrt{2\Pi\sigma_2}} \exp\left(-\frac{z^2}{2\sigma_2^2}\right), & b \leq |z|. \end{cases} \dots\dots\dots (2.4)$$

with $a = \sqrt{\frac{2\sigma_0^2\sigma_1^2}{\sigma_0^2 - \sigma_1^2} \ln\left(\frac{\sigma_0}{\sigma_1} A\right)}$, $b = \sqrt{\frac{2\sigma_1^2\sigma_2^2}{\sigma_1^2 - \sigma_2^2} \ln\left(\frac{\sigma_1}{2\sigma_2} A\right)}$

As impulsive index A becomes smaller, Eq. (2.2) sufficiently approximates Eq. (2.4). Eq. (2.4) can be considered as a simplified Class A noise model.

CHAPTER 3

MC CDMA OVER BROADBAND POWERLINE CHANNEL

Since the rapid growth of home Internet demand, high-speed data transmission on the “last mile” has become a challenging task. Nowadays, power line communications (PLC) draw increasing interest within the scientist community as a convenient and cheap alternative to already available digital subscriber line (DSL), cable or wireless technologies. Many difficulties exist, though. Electrical distribution grid constitutes an omnipresent structure but was not built for communication purposes. The power line channel exhibits multi-paths caused by reflections due to the discontinuities of the network and suffers from different types of noise among which are colored background noise, narrowband interference and the more unfavorable impulse noise. Robust and frequency efficient transmission techniques have thus to be used to cope with such a hostile channel and achieve high bit rates.

The well-known multi-carrier technique, Orthogonal Frequency Division Multiplexing (OFDM), is considered as the modulation scheme for BPL by most researchers. By the application of OFDM, the most distinct property of power-line channel, its frequency selectivity, can be easily coped with. On the other hand, Code Division Multiple-Access (CDMA) is an attractive scheme due to robustness to interferences, which is very important in BPL communications since there are two sources of interference, the interference from wireless devices and the multi-user interference in a home network.

A combination of multi-carrier modulation and CDMA, MC CDMA has the advantages of both techniques. Multi-carrier system can perform better than single carrier modulation in presence of impulsive noise, because it spreads the effect of impulsive noise over multiple sub-carriers [4]. Like other communication systems, coding can improve the multi-carrier system performance but because of the nature of this channel the achieved improvements are usually very restricted. Therefore, analysis of coded and uncoded multi-carrier communication scheme in this hostile environment seems to be necessary in

order to offer some insight about the overall performance and achievable improvements for this system.

3.1 Uncoded MC CDMA over Broadband Powerline Channel

Multiple access schemes based on a combination of CDMA and Multi-carrier modulation were first proposed in 1993 [20]. The combination of the two schemes can be done in a number of ways: MC-DS-CDMA, MT-CDMA and MC-CDMA [20] [21].

The *MC-DS-CDMA* transmitter spreads the Serial to Parallel (S/P) converted data streams using a given spreading code in the time domain so that the resulting spectrum of each sub-carrier can satisfy the orthogonality condition with the minimum frequency separation. The transmitter structure and power spectrum are shown in fig. 3.1. Here G_{MD} denotes the processing gain, N_c the number of sub-carriers and $C^j(t)$ is the spreading code of the j -th user

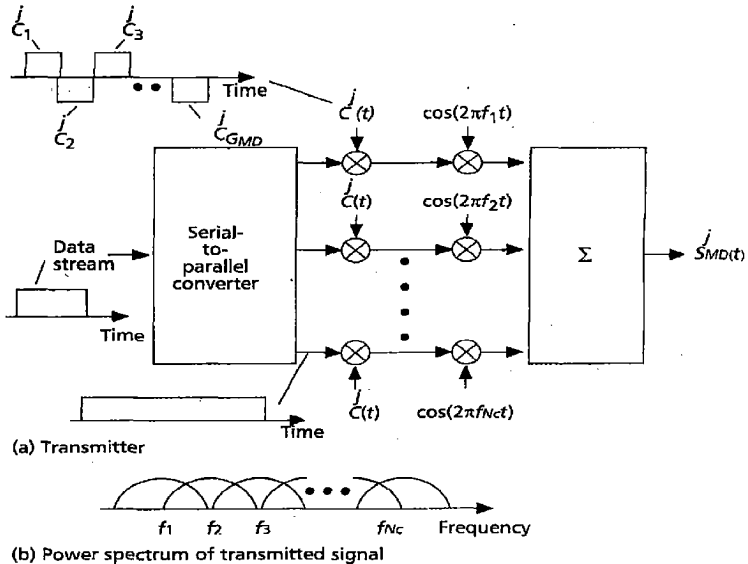


Figure 3.1 MC-DS-CDMA transmitter and power spectrum of the transmitted signal [20]

The *MT-CDMA* transmitter spreads the S/P converted data streams using a given spreading code in the time domain so that the spectrum of each sub-carrier prior to spreading operation can satisfy the orthogonality condition with the minimum frequency separation. Therefore, the resulting spectrum of each sub-carrier no longer satisfies the orthogonality condition. The *MT-CDMA* scheme uses longer spreading codes in proportion to the number of sub-carriers, as compared with a normal (single carrier) DS-CDMA scheme and therefore, the system can accommodate more users than the DS-CDMA scheme. The transmitter structure and power spectrum are shown in fig. 3.2. Here G_{MT} denotes the processing gain, N_c the number of sub-carriers and $\hat{C}^j(t)$ is the spreading code of the j -th user.

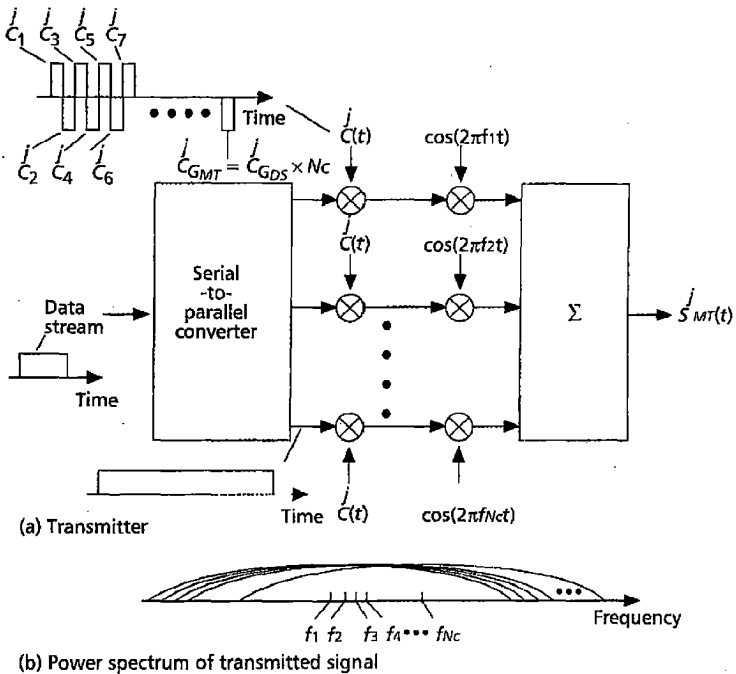


Figure 3.2 *MT-CDMA* transmitter and power spectrum of the transmitted signal [20]

The *MC-CDMA* transmitter spreads the original data stream over different sub-carriers using a given spreading code in the frequency domain. In other words, a fraction of the symbol corresponding to a chip of the spreading code is transmitted through different sub-carriers.

3.1.1 MC CDMA Transmitter

The basic transmitter structure of MC-CDMA scheme is similar to that of OFDM scheme. The main difference is that the MC-CDMA scheme transmits the same symbol in parallel through a lot of sub-carriers where as the OFDM scheme transmits different symbols [20][21].

Figure 3.3 shows the MC-CDMA transmitter of the j -th user for BPSK scheme and the power spectrum of the transmitted signal, where G_{MC} denotes the processing gain, N_c the number of sub-carriers, and $C_j(t) = [C_1^j C_2^j \dots C_{G_{MC}}^j]$ the spreading code of the j -th user. The input signal is given by

$$b_j(t) = \sum_{i=-\infty}^{+\infty} A_j b_j(i) p_s(t - iT_s)$$

The Transmitted MC-CDMA signal can be expressed as

$$S_{MC}^j(t) = \sum_{i=-\infty}^{+\infty} \sum_{n=1}^N A_j b_j(i) C_j(n) \cdot p_s(t - iT_s) \cos\{2\pi(f_0 + b\Delta f)t\}$$

Where $\Delta f (=1/T_s)$ is the sub-carrier separation, N is the multi-carrier processing gain, $C_j(n)$ is the spreading code of j 'th user at n 'th sub-carrier, A_j is the amplitude of the j 'th user, $b_j(i)$ is the original data stream at time i , $p_s(t)$ is the pulse waveform defined as

$$p_s(t) = \begin{cases} 1, & 0 \leq t \leq T_s \\ 0, & \text{otherwise} \end{cases}$$

Orthogonal codes such as Walsh Hadamard and orthogonal Gold codes which have zero cross-correlation are particularly suitable for MC-CDMA.

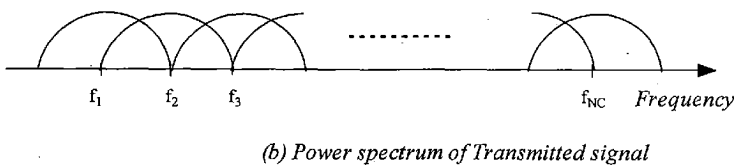
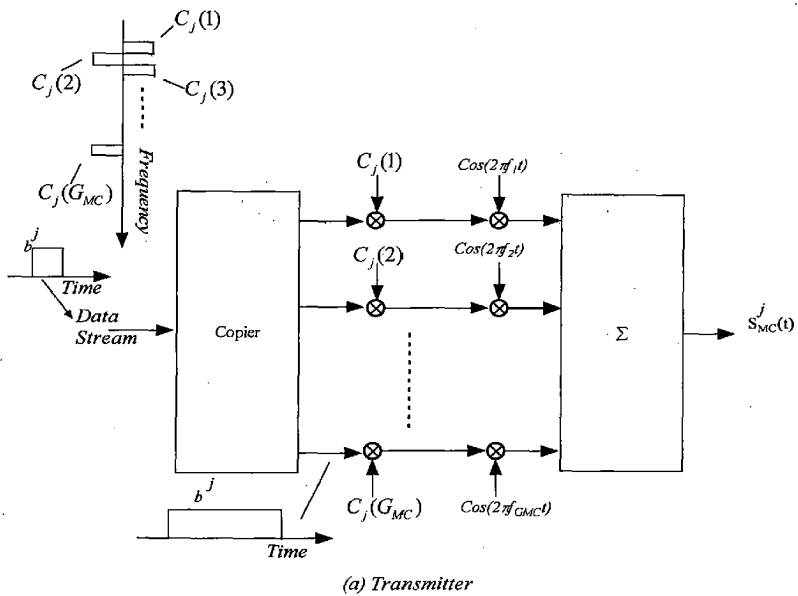


Figure 3.3 MC-CDMA transmitter and power spectrum of the transmitted signal [20]

3.1.2 MC CDMA Receiver

The main advantage of MC CDMA scheme over other schemes (DS-CDMA, MC-DS-CDMA or MT-CDMA) is that the MC-CDMA receiver can always use the full received signal energy scattered in the frequency domain to detect the desired signal [20]. Figure 3.4 shows the MC-CDMA receiver of the j '-th user, where after the serial-to-parallel conversion, the m -th sub-carrier is multiplied by the gain $q_j(G_{MC})$ to combine the received signal energy scattered in the frequency domain.

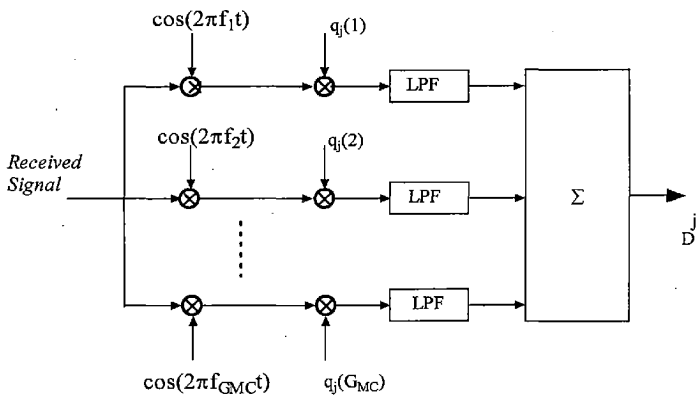


Figure 3.4 MC-CDMA receiver [20]

The received signal at the n 'th sub-carrier after down conversion is given by,

$$y(n) = \sum_{j=1}^J z_j(n) A_j b_j C_j(n) + \eta(n)$$

Where $z_j(n)$ is the complex envelope of the channel (from transmitter to the receiver) at the n 'th subcarrier for j 'th user. b_j is the complex envelope of the transmitted symbol for j 'th user and $\eta(n)$ is the noise. The channel characteristics is assumed to be same for all users, $z_j(n) = z(n)$, $j = 1, 2, \dots, J$ where J is the number of users.

Decision variable is given by

$$D^j = \sum_{m=1}^J q_j(n) y(n)$$

Where $q_j(n) = C_j(n) z(n)^*$

3.1.3 Combining Techniques [20][21]

There are different combining techniques for MC CDMA, some of these techniques are listed next.

(a) Orthogonality Restoring Combining (ORC):

Choosing the gain as $q_j(n) = C_j(n)z(n)^* / |z(n)|^2$ the receiver can eliminate the multi-user interference perfectly

$$D^j = b_j + \sum_{n=1}^{G_{MC}} C_j(n)z(n)^* / |z(n)|^2 n(n)$$

However, low-level sub-carriers tend to be multiplied by the high gains, and the noise components are amplified at weaker sub-carriers. This noise amplification effect degrades the BER performance.

(b) Equal Gain Combining (EGC):

Equal Gain combining attempts to correct the channel induced phase rotations, leaving the faded magnitudes uncorrected. In this case gain factor is given by

$$q_j(n) = C_j(n)z(n)^* / |z(n)|$$

(c) Maximum Ratio Combining (MRC):

In Maximum Ratio combining a stronger signal is assigned a higher weight by the diversity combiners, than a weaker signal, since its contribution is more reliable. The gain for MRC is given by

$$q_j(n) = C_j(n)z(n)^*$$

This equalization gain attempts to de-attenuate and de-rotate the fading induced attenuation and phase rotation. In the case of single user, the MRC can minimize the BER.

(d) Minimum Mean Square Error Combining (MMSEC):

Based on the minimum mean square estimation criterion, error must be orthogonal to all baseband components of the received sub-carriers

$$E[(b_j - \hat{b}_j) \cdot y(n)^*] = 0 \quad (n = 1, 2, \dots, K_{MC})$$

$$q_j(n) = C_j(n)z(n)^* / (J |z(m)|^2 + N)$$

For small $|z(m)|$, the gain becomes small to avoid the excessive noise amplification while for large $|z(m)|$, it becomes in proportion to the inverse of the sub-carrier envelope $z(n)^* / |z(n)|^2$ in order to recover orthogonality among users.

3.2 Coded MC CDMA over Broadband Powerline Channel

In order to ensure reliable communication in hostile environments such as power lines and to reduce the bit error rate, it is required that suitable error control strategies should be applied. There are many coding techniques available, which are known to perform better in the AWGN environment; we can apply them for Powerline channel because coding solutions closely matched to the features of the PL channel are not available. One such coding technique is Turbo coding whose performance in terms of Bit Error Rate (BER) is close to the Shannon limit [7]. Turbo coding consists of two key design innovations: parallel concatenated encoding and iterative decoding.

A Turbo encoder consists of two recursive systematic convolutional component encoders connected in parallel and separated by a random interleaver. A Turbo decoder, which is iterative, is typically based on either a *Soft Output Viterbi Algorithm* (SOVA) or a *Maximum A Posteriori* (MAP) algorithm. The iterative process performs information exchange between the two component decoders. By increasing the number of iterations in Turbo decoding, a bit error probability as low as $10^{-5} - 10^{-7}$ can be achieved at a signal to noise ratio close to the Shannon capacity limit [22].

3.2.1 Turbo Encoder [22]

A Turbo encoder is formed by parallel concatenation of two *recursive systematic convolutional* (RSC) encoders separated by a random interleaver. The encoder structure is called parallel concatenation because the two encoders operate on the same set of input bits, rather than one encoding the output of the other. Thus Turbo codes are also referred to as *parallel concatenated convolutional codes* (PCCC). A block diagram of a rate 1/3 Turbo encoder is shown in fig. 3.5. The component RSC code is a rate 1/2 code. The generator matrix of a rate 1/2 component RSC code can be represented as

$$G(D) = \begin{bmatrix} 1 & g_1(D) \\ & g_0(D) \end{bmatrix}$$

Where D represents the delay and $g_0(D)$ and $g_1(D)$ are the feedback and feed-forward polynomials respectively. The degree of these polynomials is ν , which depends on the number of delays in the convolutional encoders.

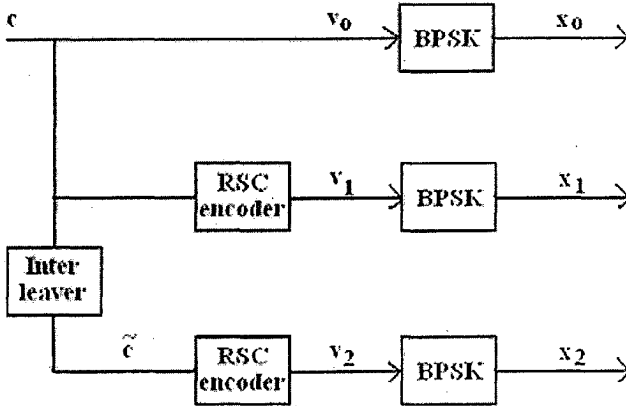


Figure 3.5 A basic Turbo encoder [22]

As shown in fig. 3.5, the same information sequence is encoded twice but in a different order. The first encoder operates directly on the input sequence, denoted by c , of length N . The first component encoder has two outputs. The first output denoted by v_0 , is equal to the input sequence since the encoder is systematic. The other output is the parity check sequence denoted by v_1 , the interleaved information sequence at the input of the second encoder is denoted by \tilde{c} . From the second encoder only the parity check sequence, denoted by v_2 , is transmitted. The information sequence v_0 and the parity check sequences of the two encoders, v_1 and v_2 are multiplexed to generate the Turbo code sequence. The overall code rate is $1/3$. The parity bits might be punctured to obtain the rate $1/2$.

In this work a rate 1/3 Turbo code encoder, based on a (2, 1, 4) RSC code, is used. The component codes are identical (2, 1, 4) RSC codes with code rate 1/2 and memory order $\nu = 4$ (the number of states is $M_s = 16$). The generator matrix of the RSC code is given by

$$\left[1 \quad \frac{1 + D^4}{1 + D^1 + D^2 + D^3 + D^4} \right]$$

The encoding operation can be modeled as a discrete time finite state Markov process. This process can be graphically represented by state and trellis diagrams. In response to the input c_t , the finite state Markov process generates an output v_t and changes its state from S_t to S_{t+1} , where $t+1$ is the next time instant. The state sequence from time 0 to t is denoted by S_0^t and is written as

$$S_0^t = (S_0, S_1, \dots, S_t)$$

The state sequence is a Markov process, so that the probability $P(S_{t+1} | S_0, S_1, \dots, S_t)$ of being in state S_{t+1} , at time $(t + 1)$, given all states up to time t , depends only on the state S_t at time t .

$$P(S_{t+1} | S_0, S_1, \dots, S_t) = P(S_{t+1} | S_t)$$

The encoder output sequence from time 1 to t is represented as

$$v_1^t = (v_1, v_2, \dots, v_t)$$

Where $v_t = (v_{t,0}, v_{t,1}, \dots, v_{t,n-1})$ is the code block of length n . The code sequence v_1^t is modulated by a BPSK modulator. The modulated sequence is denoted by x_1^t and is given by

$$x_1^t = (x_1, x_2, \dots, x_t)$$

where $x_t = (x_{t,0}, x_{t,1}, \dots, x_{t,n-1})$ and $x_{t,i} = 2 v_{t,i} - 1$, $i = 0, 1, \dots, n-1$. As there is one to one correspondence between the code and modulated sequence, the encoder/modulator pair can be represented by a discrete-time finite-state Markov process and can be graphically

described by state or trellis diagrams. The modulated sequence x_1' is corrupted by noise, resulting in the received sequence

$$r_1' = (r_1, r_2, \dots, r_t)$$

Where $r_t = (r_{t,0}, r_{t,1}, \dots, r_{t,n-1})$ and $r_{t,i} = x_{t,i} + n_{t,i}$, $i = 0, 1, \dots, n-1$, $n_{t,i}$ is memoryless noise. Each noise sample is assumed to be independent from each other. The decoder gives an estimate of the input to the discrete finite-state Markov source, by examining the received sequence r_1' .

3.2.2 Turbo Decoder [22]

Turbo codes are decoded using an iterative decoding strategy based on decoding the constituent codes, by passing information between constituent decoders. A Turbo decoder, which is iterative, is typically based on either a *Soft Output Viterbi Algorithm* (SOVA) or a *Maximum A Posteriori* (MAP) algorithm. SOVA is an extension of the classical Viterbi algorithm that accepts soft input and delivers soft output for each decoded bit. While the MAP algorithm provides the best performance in terms of minimizing the bit error rate (BER), SOVA has significantly lower complexity with only slight degradation in decoding performance [22]. In this work, iterative MAP algorithm is used for decoding the Turbo codes. An iterative Turbo code decoder based on the MAP algorithm is shown in Fig. 3.6.

Iterative Turbo decoding consists of two component decoders serially concatenated via an interleaver. The first MAP decoder takes as input the received information sequence r_0 and the received parity sequence generated by the first encoder r_1 . The decoder then produces a soft output, which is interleaved and used to produce an improved estimate of the a priori probabilities of the information sequence for the second decoder.

The other two inputs to the second MAP decoder are the interleaved received information sequence \check{r}_0 and the received parity sequence produced by the second encoder r_2 . The second MAP decoder also produces a soft output which is used to improve the estimate of the a priori probabilities for the information sequence at the input of the first MAP

decoder. The decoder performance can be improved by this iterative operation relative to a single operation serial concatenated decoder. The feedback loop is a distinguishing feature of this decoder. After a certain number of iteration the soft outputs of both MAP decoders stop to produce further performance improvements. Then the last stage of decoding makes a hard decision after de-interleaving.

3.2.2.1 Iterative MAP Algorithm [22]

MAP algorithm is used here in the iterative decoding, the first MAP decoder in the first iteration is considered first.

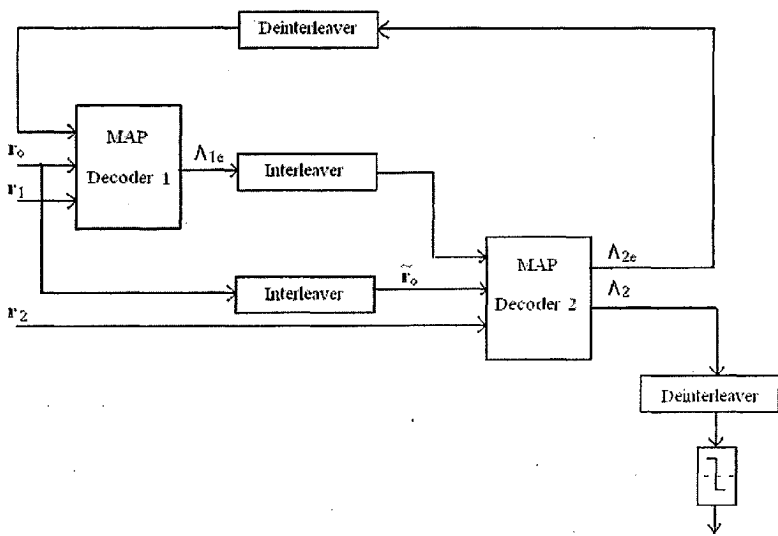


Figure 3.6 An iterative Turbo code decoder based on the MAP algorithm [22]

(i) *First MAP decoder*

The log-likelihood ratio $\Lambda_1(c_i)$ of the first MAP decoder is given by

$$\Lambda_1(c_i) = \log \left(\left(\sum_{l',j=0}^{Ms-1} \alpha_{l'-1}(l') \cdot p_i^1(1) \exp \left(-\frac{\sum_{j=0}^{n-1} (r_{i,j} - x_{i,j}^1(l'))^2}{2\sigma^2} \right) \beta_i(l') \right) / \right. \\ \left. \left(\sum_{l',j=0}^{Ms-1} \alpha_{l'-1}(l') \cdot p_i^1(0) \exp \left(-\frac{\sum_{j=0}^{n-1} (r_{i,j} - x_{i,j}^0(l'))^2}{2\sigma^2} \right) \beta_i(l') \right) \right) \quad (3.1)$$

Where $p_i^1(1)$ and $p_i^1(0)$ are the a priori probabilities for 1 and 0 at the input of the first decoder respectively, and for the second decoder these are $p_i^2(1)$ and $p_i^2(0)$. Here $\alpha_i(l) = \Pr\{S_t = l, r_t^i\}$, $\beta_i(l) = \{r_{t+1}^i | S_t = l\}$, and σ^2 is noise variance. In the initial decoding operation in the first decoder it is assumed that $p_i^1(1) = p_i^1(0) = 1/2$. Rewriting $\Lambda_1(c_i)$ as

$$\Lambda_1(c_i) = \log \frac{p_i^1(1)}{p_i^1(0)} \\ + \log \left(\left(\sum_{l',j=0}^{Ms-1} \alpha_{l'-1}(l') \cdot \exp \left(-\frac{(r_{i,0} - x_{i,0}^1)^2 + \sum_{j=1}^{n-1} (r_{i,j} - x_{i,j}^1(l'))^2}{2\sigma^2} \right) \beta_i(l') \right) / \right. \\ \left. \left(\sum_{l',j=0}^{Ms-1} \alpha_{l'-1}(l') \cdot \exp \left(-\frac{(r_{i,0} - x_{i,0}^0)^2 + \sum_{j=1}^{n-1} (r_{i,j} - x_{i,j}^0(l'))^2}{2\sigma^2} \right) \beta_i(l') \right) \right)$$

Where $(n-1)$ is the number of parity digits in the encoded block. Since the code is systematic $x_{i,0}^1, i = 0, 1$, are independent of the trellis and state l . That is $x_{i,0}^1 = 1$ and $x_{i,0}^0 = -1$. $\Lambda_1(c_i)$ could be further decomposed into

$$\Lambda_1(c_i) = \log \frac{p_i^1(1)}{p_i^1(0)} + \frac{2}{\sigma^2} r_{i,0} + \Lambda_{1e}(c_i) \quad (3.2)$$

$$\text{Where } \Lambda_{1e}(c_i) = \log \left(\left(\sum_{l',j=0}^{Ms-1} \alpha_{l'-1}(l') \cdot \exp \left(-\frac{\sum_{j=1}^{n-1} (r_{i,j} - x_{i,j}^1(l'))^2}{2\sigma^2} \right) \beta_i(l') \right) / \right. \\ \left. \left(\sum_{l',j=0}^{Ms-1} \alpha_{l'-1}(l') \cdot \exp \left(-\frac{\sum_{j=1}^{n-1} (r_{i,j} - x_{i,j}^0(l'))^2}{2\sigma^2} \right) \beta_i(l') \right) \right)$$

$\Lambda_{1e}(c_i)$ is called the *extrinsic information*. It is a function of the redundant information introduced by the encoder. It does not contain the information decoder input $r_{i,0}$. This

quantity may be used to improve the a priori probability estimate for the next decoding stage.

(ii) Second MAP decoder

Since the input to the second decoder includes the interleaved version of \mathbf{r}_0 , the received information signal $\tilde{r}_{t,0}$ correlates with the interleaved soft output from the first decoder, $\tilde{\Lambda}_1(\mathbf{c}_t)$. Therefore the contribution due to $r_{t,0}$ must be taken out from $\Lambda_1(\mathbf{c}_t)$, to eliminate this correlation. However $\Lambda_{1e}(\mathbf{c}_t)$ does not contain $r_{t,0}$ and it can be used as the a priori probability for decoding in the second stage. That is, the interleaved extrinsic information of the first decoder $\tilde{\Lambda}_{1e}$ is the a priori probability estimate for the second decoder.

$$\tilde{\Lambda}_{1e}(\mathbf{c}_t) = \log \frac{p_t^2(1)}{p_t^2(0)}$$

In the second decoding stage the MAP decoder estimates the log-likelihood ratio $\Lambda_2(\mathbf{c}_t)$. Similarly to eq (3.2) the log-likelihood ratio for the second MAP decoder can be decomposed into

$$\Lambda_2(\mathbf{c}_t) = \log \frac{p_t^2(1)}{p_t^2(0)} + \frac{2}{\sigma^2} \tilde{r}_{t,0} + \Lambda_{2e}(\mathbf{c}_t) \quad \dots\dots\dots(3.3)$$

$$\Lambda_2(\mathbf{c}_t) = \tilde{\Lambda}_{1e}(\mathbf{c}_t) + \frac{2}{\sigma^2} \tilde{r}_{t,0} + \Lambda_{2e}(\mathbf{c}_t) \quad \dots\dots\dots(3.4)$$

$\Lambda_{2e}(\mathbf{c}_t)$ is the extrinsic information for the second decoder, which depends on the redundant information supplied by the second encoder. The second decoder extrinsic information can be used as the estimates of the a priori probabilities for the first decoder. The log-likelihood ratio for the first MAP decoder can be written as

$$\Lambda_1(\mathbf{c}_t) = \tilde{\Lambda}_{2e}(\mathbf{c}_t) + \frac{2}{\sigma^2} \tilde{r}_{t,0} + \Lambda_{1e}(\mathbf{c}_t) \quad \dots\dots\dots(3.5)$$

3.2.2.2 Algorithm steps of Iterative MAP Decoding Method

- i. Initialize $\Lambda_{2e}^{(0)}(\mathbf{c}_t) = 0$.
- ii. For iterations $r = 1, 2, \dots, I$, where I is the total no of iterations

- Compute $\Lambda_1^{(r)}(c_t)$ and $\Lambda_2^{(r)}(c_t)$ by using eq. (3.11.a)
- Compute $\Lambda_{1e}^{(r)}(c_t)$ as

$$\Lambda_{1e}^{(r)}(c_t) = \Lambda_1^{(r)}(c_t) - \frac{2}{\sigma^2} r_{t,0} - \tilde{\Lambda}_{2e}^{(r-1)}(c_t) \quad \dots\dots\dots(3.6)$$

- Compute $\Lambda_{2e}^{(r)}(c_t)$ as

$$\Lambda_{2e}^{(r)}(c_t) = \Lambda_2^{(r)}(c_t) - \frac{2}{\sigma^2} \check{r}_{t,0} - \tilde{\Lambda}_{2e}^{(r)}(c_t) \quad \dots\dots\dots(3.7)$$

iii. After I iterations make a hard decision on c_t based on $\tilde{\Lambda}_2^{(I)}(c_t)$.

3.3 Performance of Uncoded and Coded MC-CDMA over BPL

In this section performance of uncoded and coded MC CDMA over broadband powerline channel is discussed on the basis of results available in the literature so far. Very few results are known so far, which include performance of Convolutional codes, Hamming codes and Golay codes with MC CDMA over BPL. In ref [23], authors presented the performance of uncoded MC CDMA over BPL. Two noise models viz. Markov based model and Middleton's model are used for simulation and the performance in terms of interleaver size is also given. Figure 3.7 and 3.8 shows the performance of uncoded and coded MC CDMA over PBL.

Performances of coded MC CDMA using (7,4) Hamming codes, (23,12) Cyclic Golay codes and (3,1) Convolutional codes are given in [24] for PLC. Convolutional codes have been shown to perform the best among the above codes. The simulation results of ref. [24] are shown in figure 3.9 and 3.10. LDPC codes perform better in comparison to Reed-Solomon codes and Convolutional codes for higher SNR values [25]. For lower SNR the performance of above three coding schemes is comparable. BPSK modulation scheme and OFDM transmission technique with 512 sub-carriers were used in the study.

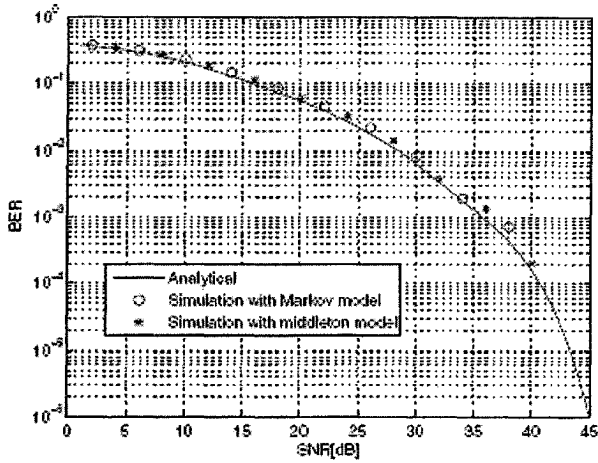


Figure 3.7 Uncoded MC CDMA over impulsive noise frequency selective channel [23]

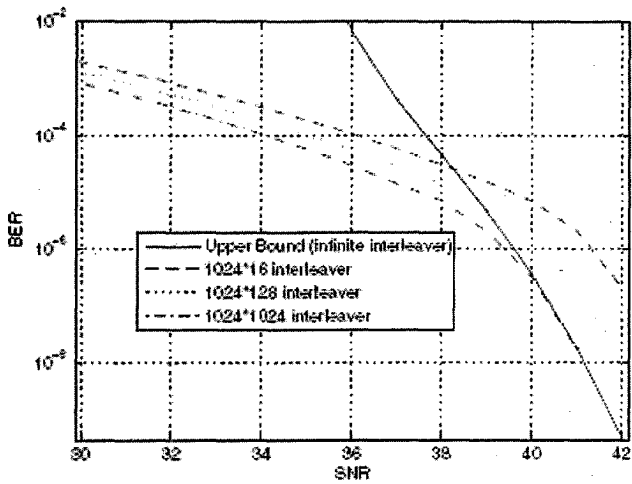


Figure 3.8 Coded MC CDMA with different interleaver size [23]

This chapter describes the system model that has been used in this dissertation work to find the performance of Turbo coded MC CDMA over broadband powerline channel. It also includes the flow-chart of the simulation work. MATLAB 7.2.0.232 (R2006a) is used as the simulation tool.

4.1 System Model

The system model includes a Turbo encoder for encoding the user's data, and then this coded data is passed through a BPSK modulator. Now this data is passed through a MC CDMA transmitter, which includes the operation of spreading, serial to parallel conversion, IFFT and again parallel to serial conversion. After this the modulated data is passed through the powerline channel. At the receiver side data is passed through the MC CDMA receiver, where serial to parallel conversion, FFT, despreading and combining operations take place. This is followed by BPSK demodulator and the signal is finally decoded using iterative MAP algorithm. The system model is shown in fig. 4.1.

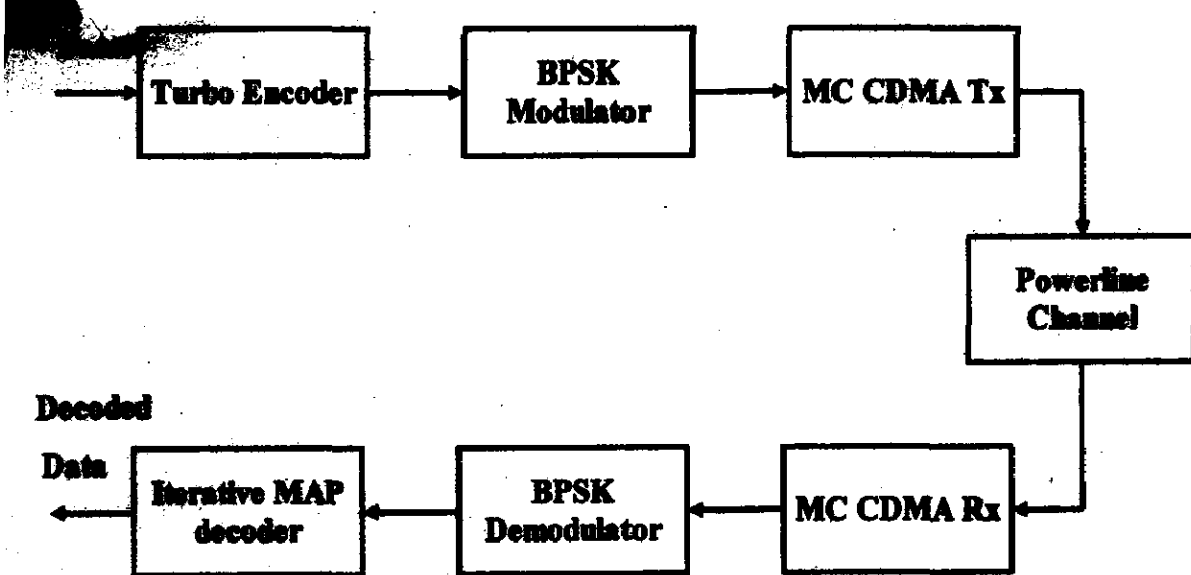


Figure 4.1 Coded MC CDMA over broadband PLC

4.2 Powerline Channel

The channel model proposed by Zimmermann and Dostert [9] has been used for the simulation. The transfer function of the channel is

$$H(f) = \sum_{i=1}^N g_i \exp(-(a_0 + a_i f^k) d_i) \exp(-j2\pi f \tau_i)$$

Here N is the number of relevant propagation paths, a_0 and a_i are link attenuation parameters, k is an exponent (with typical values ranging from 0.5 to 1), g_i is the weighting factor for path i , d_i its length, and τ_i its delay. The values of these parameters used in the simulation are given in Table 4.1 and Table 4.2 for $N=15$ propagation paths and $N=4$ propagation paths respectively. For all the users, the channel is assumed to be the same. The channel model is simulated and the flow-chart is shown in fig 4.2.

Attenuation Parameters					
$k=1$	$a_0=0$	$a_i = 7.8 * 10^{-10}$ m/s			
Path Parameters					
i	g_i	$d_i(m)$	i	g_i	$d_i(m)$
1	0.029	90	9	0.071	411
2	0.043	102	10	-0.035	490
3	0.103	113	11	0.065	567
4	-0.058	143	12	-0.055	740
5	-0.045	148	13	0.042	960
6	-0.040	200	14	-0.059	1130
7	0.038	260	15	0.049	1250
8	-0.038	322			

Table – 4.1 Parameters of a 15 path model [9]

Attenuation Parameters		
k=1	a ₀ = 0	a ₁ = 7.8 * 10 ⁻¹⁰ m/s
Path Parameters		
i	g _i	d _i (m)
1	0.64	200
2	0.38	222.4
3	-0.15	244.8
4	0.05	267.5

Table – 4.2 Parameters of a 4 path model [9]

4.3 Impulsive Noise

To study the effects of impulsive noise on coded MC-CDMA system performance, the noise is generated using the Middleton’s Class A noise model [19]. According to this model the probability density function (PDF) of Class A noise is given by

$$P_{A,\Gamma,\sigma^2}(z) = \sum_{m=0}^{\infty} \frac{e^{-A} A^m}{m!} \frac{1}{\sqrt{2\pi\sigma_m}} \exp\left(-\frac{z^2}{2\sigma_m^2}\right)$$

$$\text{with } \sigma_m^2 = \sigma^2 \frac{m/A + \Gamma}{1 + \Gamma}$$

A is the impulsive index which is defined as the product of the average number of impulses reaching the receiver in the time unit and the mean duration of the impulses. In this simulation A is taken as 0.01. Another parameter $\Gamma = (\sigma^2_G/\sigma^2_I)$ is the Gauss-to-impulsive noise power ratio and its value is taken as 0.01. This means that when impulse occurs, power of the noise is raised to 20 dB above normal level. The noise model is simulated and the flow-chart is shown in fig. 4.3.

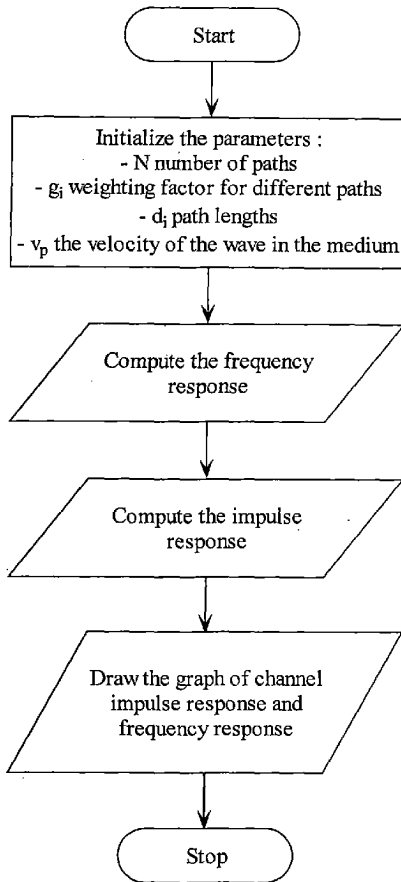


Figure 4.2 Flow-chart for the simulation of channel model

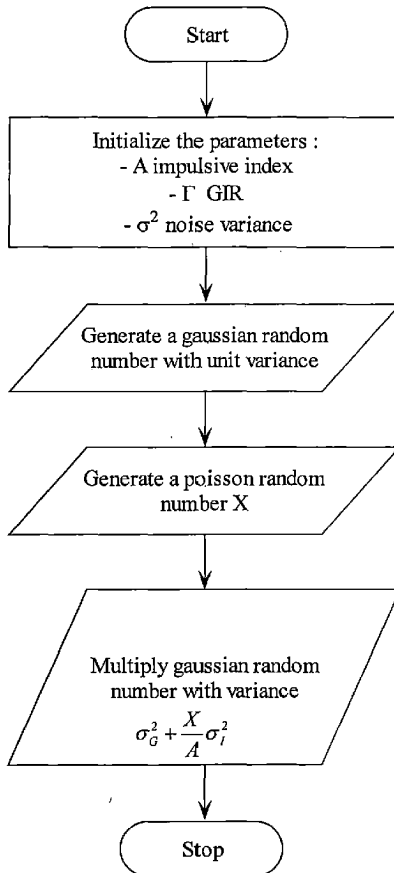


Figure 4.3 Flow chart for the simulation of noise

4.4 System parameters for the Coded MC CDMA

Powerline channel has been simulated in the frequency range 0.5 to 18 MHz. The channel sampling rate is taken as 40 MHz. The delay spread of the channel is 2 microseconds. To avoid ISI and ICI, OFDM symbol interval is taken 10 times the delay spread, which is equal to 20 microseconds. By considering 16 MHz bandwidth, the system is designed

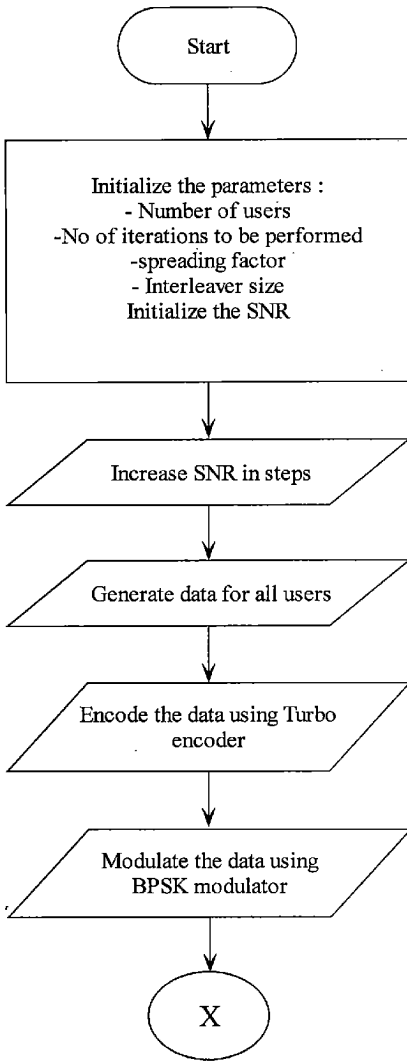
with 256 sub-carriers. Walsh Hadmard codes, with spreading factor 256, are used for spreading the data. A rate 1/3 turbo code encoder, based on a (2, 1, 4) RSC code, is used for encoding the data. The component codes are identical (2, 1, 4) RSC codes with code rate 1/2 and memory order $\nu = 4$ (the number of states is $M_s = 16$). The generator matrix of the RSC code is given by

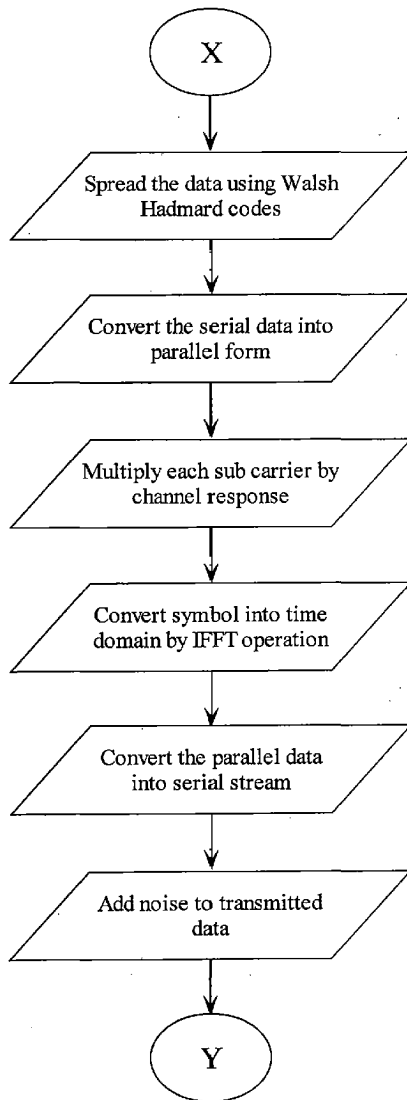
$$G(D) = \left[1 \quad \frac{1+D^4}{1+D^1+D^2+D^3+D^4} \right]$$

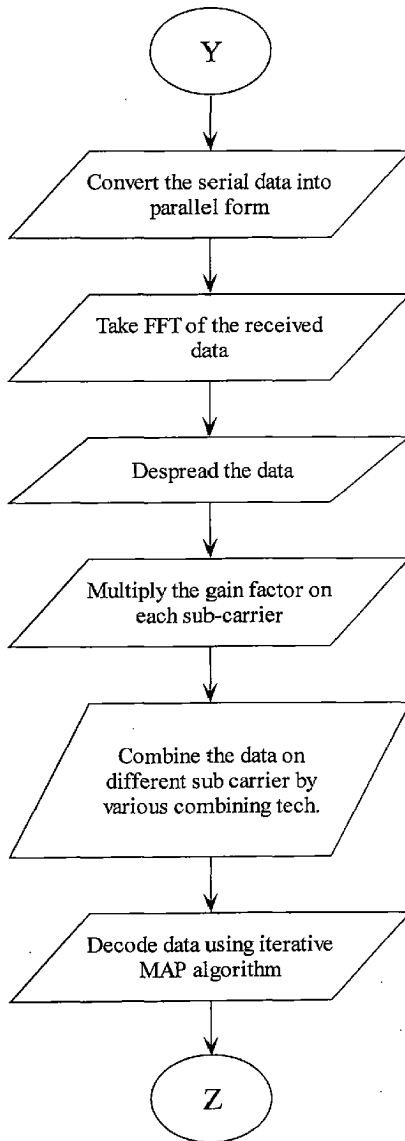
Block interleaver of size 100 is used for interleaving the data in the turbo encoder. In this interleaver data is written in a matrix row wise and read out column wise. For decoding the data iterative MAP algorithm is used. Hard decision is taken after 4 iterations. Table 4.3 lists all the parameters used in the simulation. The system is simulated and the flow-chart is shown in fig. 4.4.

Bandwidth	16 MHz
Delay spread	2 μ sec
Spreading code	Walsh Hadmard
No of sub carriers	256
Spreading factor	256
FFT size	256
Modulation	BPSK
Coding scheme	Turbo codes (rate 1/3)
Turbo encoder	(21,37) based on (2,1,4) RSC code
Decoding algorithm	Iterative MAP algorithm
Interleaver used in turbo codes	Size 100, Block interleaver

Table – 4.3 Parameters of Coded MC CDMA system







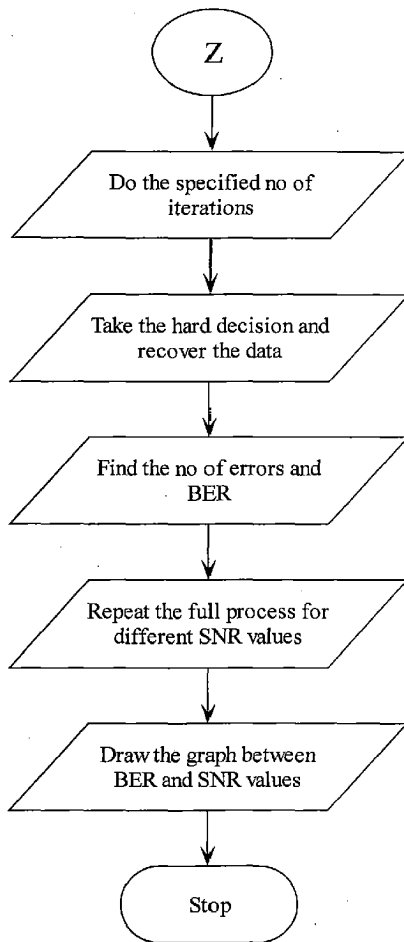


Figure 4.4 Flow chart of the simulation of the system model

RESULTS & DISCUSSION

The results obtained through computer simulation are discussed in this chapter. The BER performance of Turbo codes combined with MC-CDMA over broadband powerline channel is evaluated for single user and multi-user case. This performance is compared with that of uncoded MC-CDMA system obtained through simulation and with other reported results for (7,4) Hamming codes, (23,12) Cyclic golay codes and (3,1) Convolution codes qualitatively. The effect of different combining techniques such as MRC, EGC, ORC and MMSEC on the performance is also examined.

5.1 Channel Model

Frequency response and impulse response of the simulated channel for $N=15$ and $N=4$ are shown in figs. 5.1 and 5.2 respectively. Simulated channel model is similar to the reference model given by Zimmermann and Dostert [9].

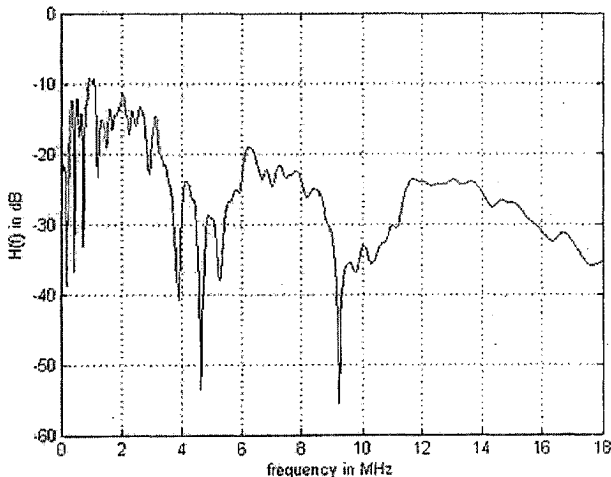


Figure 5.1 (a) Frequency response of 15-path simulated channel model

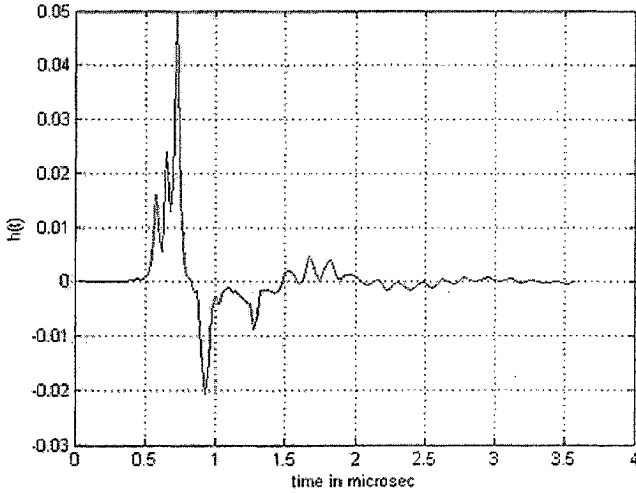


Figure 5.1 (b) Impulse response of 15 path simulated channel model

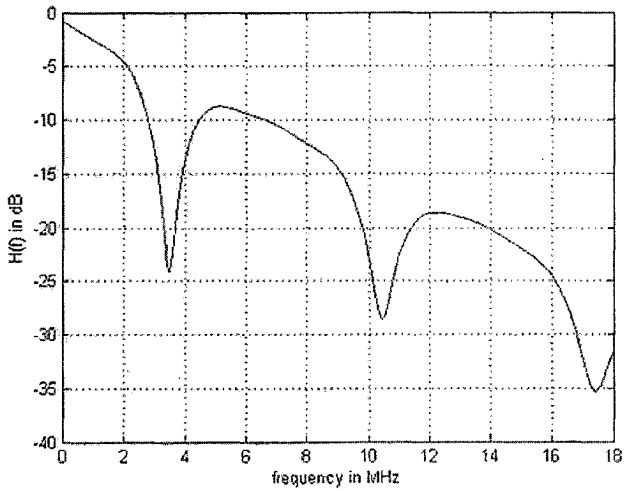


Figure 5.2 (a) Frequency response of 4 path simulated channel model

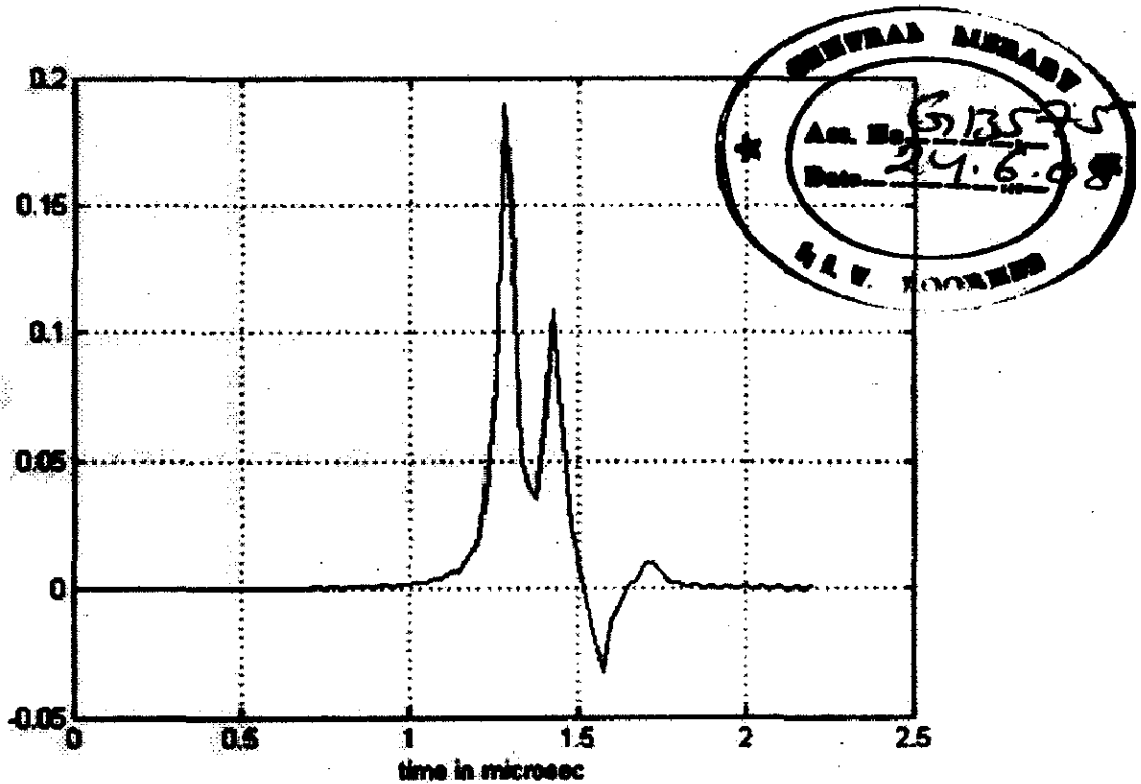


Figure 5.2 (b) Impulse response of 4 path simulated channel model

5.2 Impulsive Noise Model

Middleton's class A noise model is simulated for two different values of A. Simulation results are shown in figs. 5.3 (a) and (b). It can be seen from fig 5.3 that noise is more structured (impulsive) for small values of A, and less structured (approximately Gaussian) for large values of A.

5.3 Performance of Turbo coding in Impulsive Noise Environment

Figure 5.4 shows the BER performance of Turbo coding in the presence of impulsive noise ($A=0.01$, $\Gamma=0.01$). BPSK modulation is used in this simulation. Performance of Turbo codes in AWGN environment is well known [22]. But in impulsive noise, it can be seen that performance degrades.

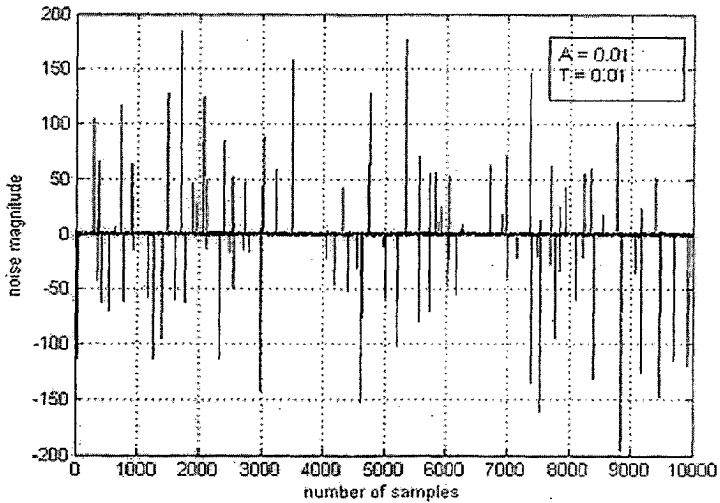


Figure 5.3 (a) simulated noise model for $A=0.01$

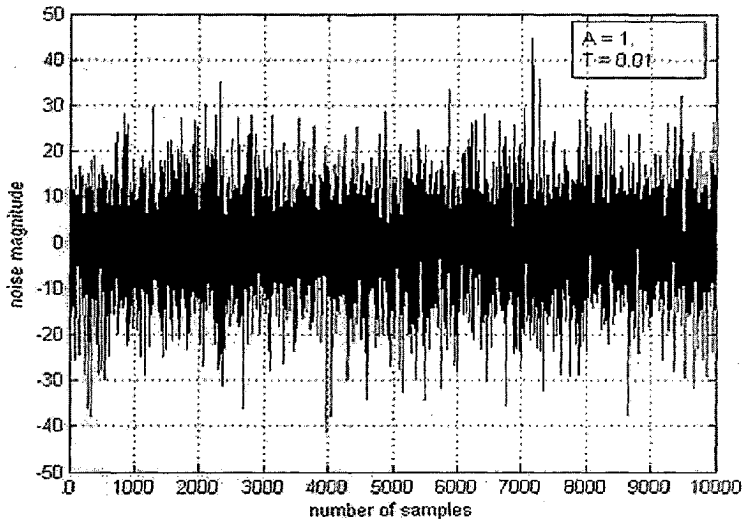


Figure 5.3 (b) simulated noise model for $A = 1$

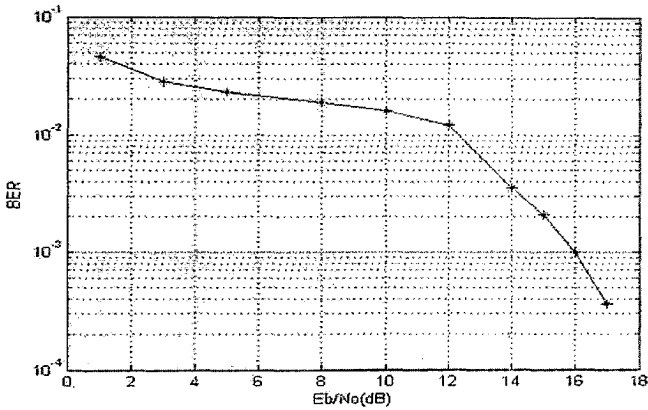


Figure 5.4 BER performance of Turbo coding in impulsive noise

5.4 Performance of MC-CDMA over BPL with Impulsive Noise

Performance of MC-CDMA is evaluated over broadband powerline channel with impulsive noise. MRC, EGC, ORC and MMSEC combining techniques are used and results are shown in figure 5.5 to 5.8. All results are taken for single user and eight users. Relative performance of all for combining techniques closely matches with the well known standard results [21]. A representative performance comparison for MC-CDMA over BPL is given in Table - 5.1.

BER at $E_b/N_0 = 10\text{dB}$				
	MRC	EGC	ORC	MMSEC
Single user	9×10^{-4}	7.1×10^{-3}	9×10^{-2}	6.3×10^{-2}
Eight users	1.7×10^{-2}	2.8×10^{-2}	2.7×10^{-1}	2.2×10^{-1}
BER at $E_b/N_0 = 20\text{dB}$				
	MRC	EGC	ORC	MMSEC
Single user	$< 10^{-4}$	1.4×10^{-3}	1.7×10^{-2}	1.5×10^{-2}
Eight users	9.1×10^{-4}	6×10^{-3}	1×10^{-1}	1×10^{-1}

Table - 5.1 BER performance comparisons for MC-CDMA over BPL

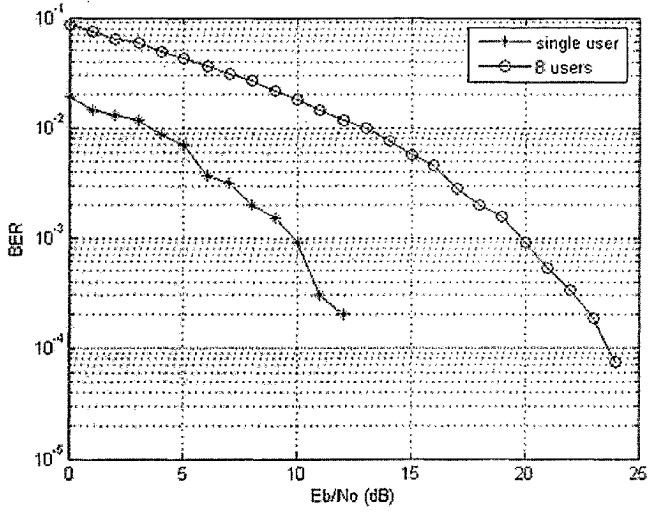


Figure 5.5 BER performance of MC-CDMA with MRC

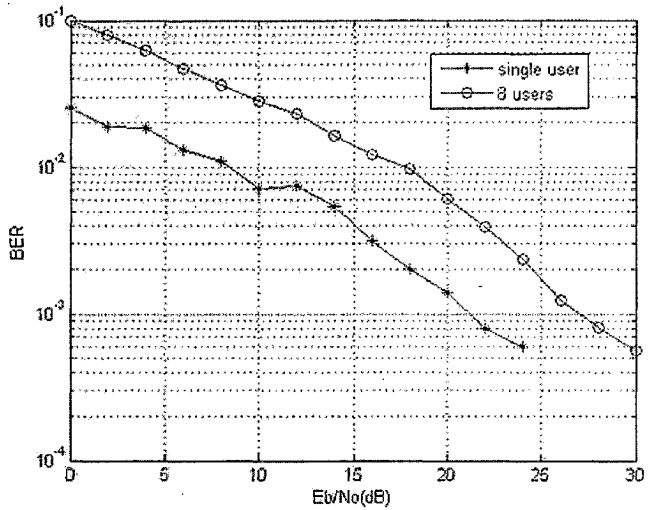


Figure 5.6 BER performance of MC-CDMA with EGC

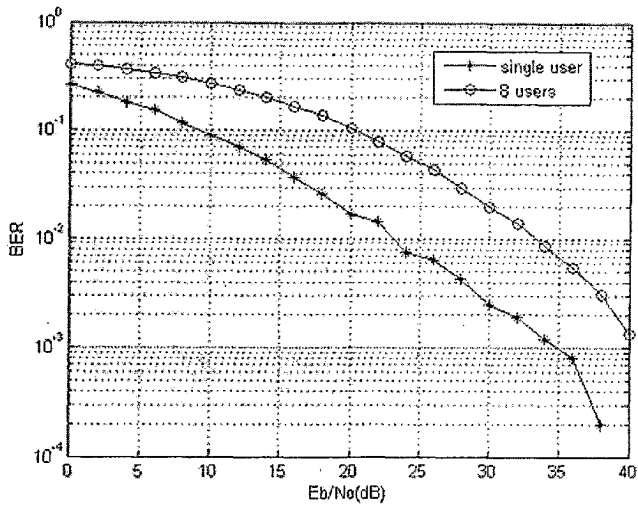


Figure 5.7 BER performance of MC-CDMA with ORC

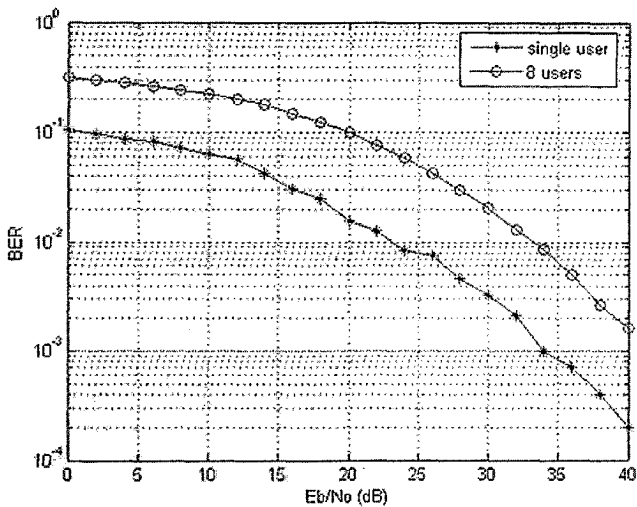


Figure 5.8 BER performance of MC-CDMA with MMSE

5.5 Performance of Turbo Coded MC-CDMA over BPL with Impulsive Noise

The performance of Turbo coded MC-CDMA over broadband powerline channel with impulse noise is shown in figure 5.9 to 5.12. The performance is evaluated for single user and eight users scenario with different combining techniques and representative performance comparisons are given in Table - 5.2. Channel is assumed same for all the users. When these results are compared with the uncoded MC-CDMA over BPL (Table - 5.1), the advantage of Turbo coding can be seen. For example, a BER of 3×10^{-4} at 10dB Eb/No is achieved with Turbo coded system in comparison with BER of 7.1×10^{-3} with uncoded system in the same conditions.

BER at Eb/No = 8dB				
	MRC	EGC	ORC	MMSEC
Single user	$< 10^{-4}$	6×10^{-4}	1.5×10^{-1}	7×10^{-2}
Eight users	8×10^{-4}	1.9×10^{-2}	4×10^{-1}	3.5×10^{-1}
BER at Eb/No = 10dB				
	MRC	EGC	ORC	MMSEC
Single user	$< 10^{-4}$	3×10^{-4}	1.1×10^{-1}	5.3×10^{-2}
Eight users	$< 10^{-3}$	9.3×10^{-3}	3.6×10^{-1}	3.4×10^{-1}
BER at Eb/No = 20dB				
	MRC	EGC	ORC	MMSEC
Single user	$< 10^{-4}$	$< 10^{-4}$	1.5×10^{-3}	2×10^{-3}
Eight users	$< 10^{-4}$	1.3×10^{-4}	1.3×10^{-1}	1.3×10^{-1}
BER at Eb/No = 25dB				
	MRC	EGC	ORC	MMSEC
Single user	$< 10^{-4}$	$< 10^{-4}$	3.3×10^{-4}	3×10^{-4}
Eight users	$< 10^{-4}$	$< 10^{-4}$	1×10^{-2}	9.6×10^{-3}

Table - 5.2 BER performance comparisons for Turbo-coded MC-CDMA over BPL

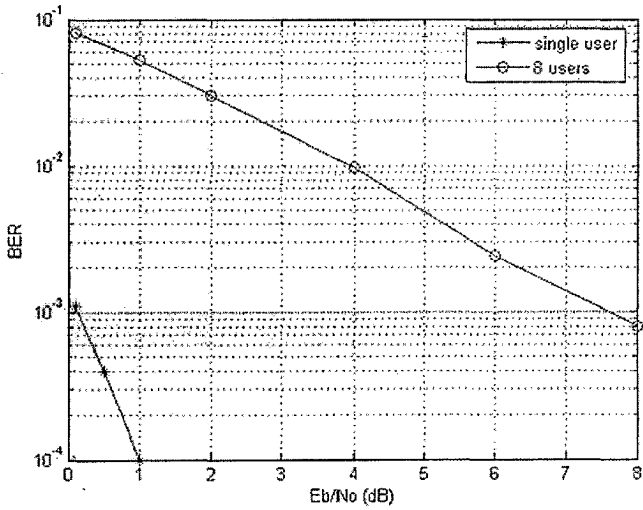


Figure 5.9 BER performance of Turbo-coded MC-CDMA with MRC

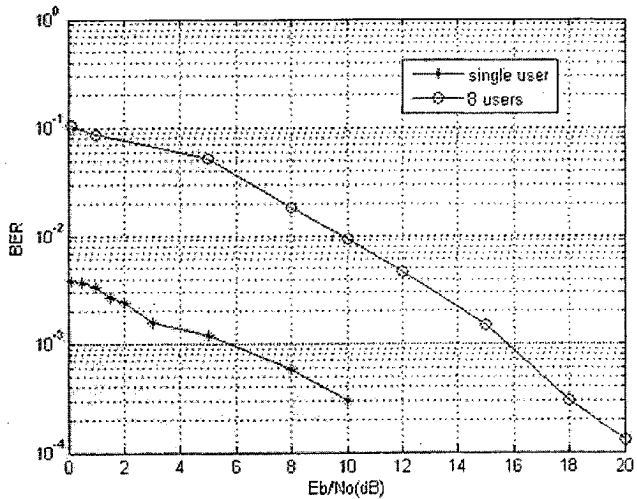


Figure 5.10 BER performance of Turbo-coded MC-CDMA with EGC

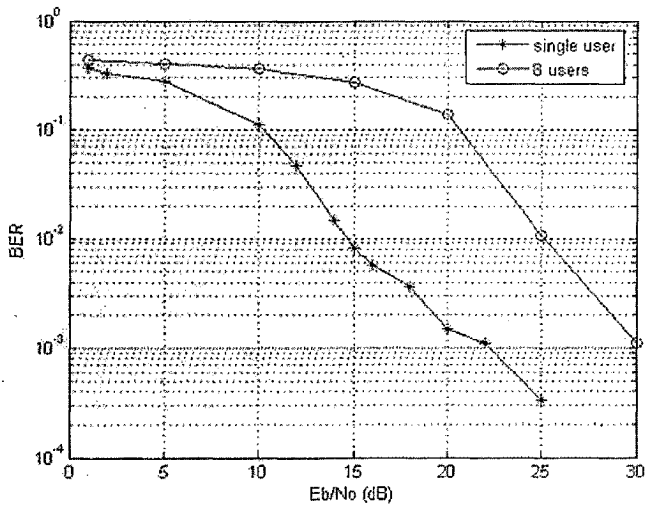


Figure 5.11 BER performance of Turbo-coded MC-CDMA with ORC

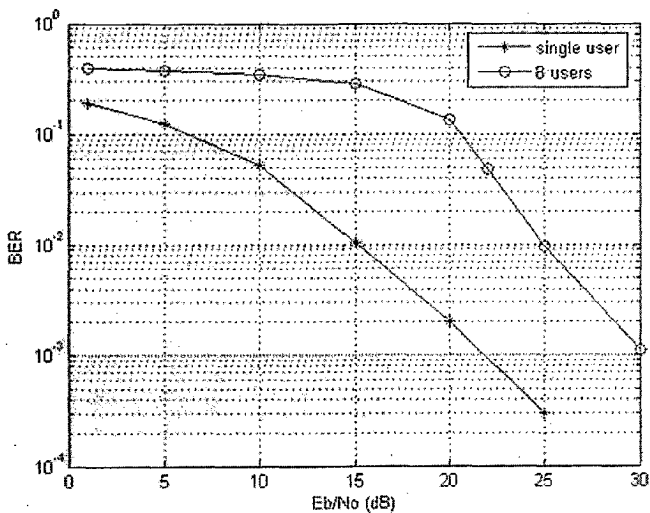


Figure 5.12 BER performance of Turbo-coded MC-CDMA with MMSEC

5.6 Performance Comparison of Turbo Coded MC-CDMA with other Coding Techniques

Very few results are available for coded MC-CDMA over BPL in literature. In ref [24], authors evaluated the performance of coded MC-CDMA over BPL using 16 sub-carriers, BPSK modulation and ORC combining for the (7,4) Hamming codes, (23,12) Cyclic Golay code and (3,1) Convolutional codes. The results are shown in fig 3.9, which is reproduced here as fig.5.13. A perusal of the results shows that a BER of 10^{-3} is achieved at 38dB, 30dB and 28 dB for the Hamming code, Cyclic Golay code and Convolutional code respectively and with interleaving the same performance is achieved at 33dB, 24dB and 23.5dB respectively, as shown in fig 3.10. In comparison, for the present work with Turbo coded MC-CDMA, the same BER is achieved at 22dB for 256 sub-carriers using BPSK modulation and ORC combining, as shown in fig 5.11.

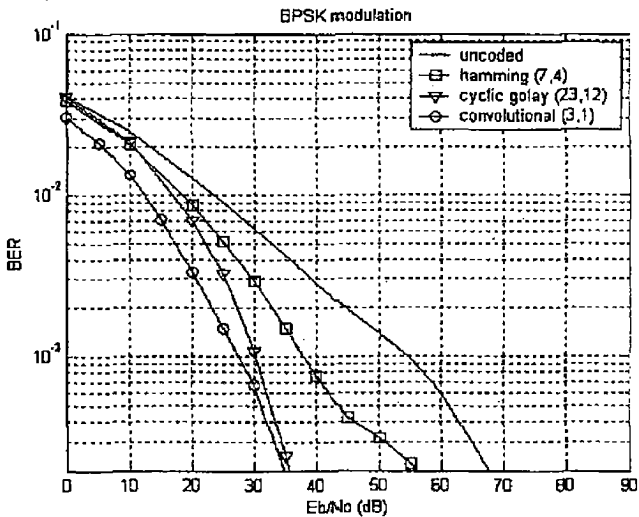


Figure 5.13 BER performance of coded MC-CDMA (BPSK modulation) [24]

CONCLUSION

In this dissertation work, Turbo coded MC-CDMA system is simulated to evaluate the performance in the powerline channel environment. The impulsive noise characteristics and channel models have also been studied and appropriate model is chosen. It can be seen from the results that use of coding improves the system BER performance. This study shows that Turbo codes perform better than Convolutional codes, Hamming codes and Cyclic Golay codes [24] for MC-CDMA over BPL. As expected, the performance degrades with increasing number of users for all the combining techniques. The degradation is least for ORC because orthogonality among different users is maintained.

From the results it is clear that high SNRs are required to attain a respectable BER, otherwise this transmission scheme performs poorly. However, the advantage of wireline nature and ubiquity of BPL may offset the power disadvantage. For practical applications of PLC, Turbo codes can be standardized due to their good performance, but the cost is paid in terms of high decoding complexity.

6.1 Scope for Future Work

The power line communication field still constitutes an open and attractive research area. More studies are still needed to better understand and improve the performance of power lines for high-bit-rate transmission. So far measurements, modeling, and transmission techniques have been the first priority in the activities of the investigators in the area, but now a stimulus in enhanced performance, coding, MAC protocols and applications is being noticed. The lack of centralized standardization and regulation is another major factor which should be overcome to facilitate the deployment.

Some immediate extensions of the present work are possible:

- (i) Other schemes such as space-time block codes can be used to take advantage of the spatial diversity intrinsic in the use of a three-phase

powerline; performance of LDPC and serial concatenated codes can also be evaluated for BPL environment.

- (ii) Performance of MAC protocol can be evaluated for the power line channel.
- (iii) Multi-user detection techniques can also be used to evaluate the performance.

REFERENCES

- [1] S. Gali, A. Scaglione, and K. Dostert, "Guest Editorial – Broadband is power: Internet access through the power line network," *IEEE Communications Magazine*, pp. 82-83, May 2003.
- [2] S. Gali, E. Biglieri, Y. H. Lee, H. V. Poor, and A. J. H. Vinck, "Guest Editorial Power Line Communication," *IEEE Journal on Selected Areas in Communications*, vol. 24, no. 7, pp. 1261-1266, July 2006.
- [3] N. Pavlidou, A. J. H. Vinck, J. Yazdani, and B. Honary, "Power line communications: state of the art and future trends," *IEEE Communications Magazine*, pp. 34-40, April 2003.
- [4] H. Dai, and H. V. Poor, "Advanced signal processing for power line communications," *IEEE Communications Magazine*, pp. 100-107, May 2003.
- [5] E. Biglieri, "Coding and modulation for a horrible channel," *IEEE Communications Magazine*, pp. 92-98, May 2003.
- [6] John A. C. Bingham, "Multicarrier Modulation for Data Transmission: An idea whose time has come," *IEEE Communications Magazine*, pp. 5-14, May 1990.
- [7] C. Berrou, A. Glavieux, and P. Thitimajshima, "Near Shannon limit error correcting coding and decoding: Turbo-codes (1)," in *Proc. IEEE ICC'93*, Geneva, Switzerland, pp. 1064–1070, May 1993.
- [8] E. Liu, G. Yangpo, G. Samdani, O. Mukhtar, and T. Korhonen, "Broadband powerline channel and capacity analysis," *Proc. Int'l. Symp. Power Line Communication and Its Applications (ISPLC'2005)*, pp. 7- 11, April 6-8, 2005.
- [9] M. Zimmermann, and K. Dostert, "A multipath model for the powerline channel," *IEEE Trans. Communication*, vol. 50, pp. 553-559, April 2002.
- [10] O. Hooijen, "A channel model for the residential power circuit used as a digital communications medium," *IEEE Trans. Electromagnetic Compatibility*, vol. 40, pp. 331-336, Nov. 1998.
- [11] S. Galli, and T. C. Banwell, "A Deterministic Frequency-Domain Model for the Indoor Power Line Transfer Function," *IEEE Journal on Selected Areas in Communications*, vol. 24, no. 7, pp.1304-1316, July 2006.

- [12] T. Sartenaer, and P. Delogne, "Deterministic Modeling of the (Shielded) Outdoor Power Line Channel Based on the Multiconductor Transmission Line Equations," *IEEE Journal on Selected Areas in Communications*, vol. 24, no. 7, pp.1277-1291, July 2006.
- [13] S. Barmada, A. Musolino, and M. Raugi, "Innovative Model for Time-Varying Power Line Communication Channel Response Evaluation," *IEEE Journal on Selected Areas in Communications*, vol. 24, no. 7, pp. 1317-1326, July 2006.
- [14] P. Karols, K. Dostert, G. Griepentrog, and S. Huettinger, "Mass Transit Power Traction Networks as Communication Channels," *IEEE Journal on Selected Areas in Communications*, vol. 24, no. 7, pp. 1339-1350, July 2006.
- [15] C. J. Hatziaioniu, N. B. Harp, and A. J. Sugg, "Finite-Element Models for Open-Air Power Lines in Broadband PLC," *IEEE Trans. Power delivery*, vol. 21, issue 4, pp. 1898-1904, Oct. 2006.
- [16] Zheng Tao, Yang Xiaoxian, and Zhang Baohui, "Broadband Transmission Characteristics for Power-Line Channels," *IEEE Trans. Power delivery*, vol. 21, issue 4, pp. 1905-1911, Oct. 2006.
- [17] M. Zimmermann, and K. Dostert, "Analysis and modeling of impulsive noise in broadband powerline communications," *IEEE trans Electromagn. Compat.*, vol. 44, pp. 249-258, Feb. 2002.
- [18] H. Hrasnica, A. Haidine, and R. Lehnert, "Broadband Powerline Communications Networks – Network Design," John Wiley & Sons Ltd, 2004.
- [19] D. Middleton, "Statistical-Physical Models of Electromagnetic Interference," *IEEE Trans. Electromagn. Compat.*, volume EMC-19, issue 3, part 1, vol. 44, pp. 106-127, Aug. 1977.
- [20] R. Prasad, and S. Hara, "Overview of Multicarrier CDMA," *IEEE Communications Magazine*, pp. 126-33, Dec. 1997.
- [21] L. Hanzo, M. Munster, B. J. Choi, and T. Keller, "OFDM and MC CDMA for Broadband Multi-User Communications - WLANs and Broadcasting," John Wiley and IEEE press, 2003.
- [22] B. Vucetic, and J. Yuan, "Turbo Codes - Principles and Applications," Kluwer Academic Publishers, 2001.

- [23] S. M. Navidpour, P. Amirshahi, and M. Kavehrad, "Performance Analysis of Coded MC-CDMA in Powerline Communication Channel with impulsive Noise," *Proc. Int'l. Symp. Power Line Commun. and Its Appl. (ISPLC'2006)*, pp. 267 – 272 March 26-29, 2006.
- [24] P. L. Katsis, G.D. Papadopoulos, and F. N. Pavlidou, "Coded MC-CDMA systems for power line communications," *Telecommunications in Modern Satellite, Cable and Broadcasting Service, 2003 (TELSIKS 2003)*, vol. 1, pp. 153 – 156, Oct. 1-3 2003.
- [25] N. Andreadou, C. Assimakopoulos, and F. N. Pavlidou, "Performance Evaluation of LDPC Codes on PLC Channel Compared to Other Coding Schemes," *Int'l. Symp. Power Line Commun. and Its Appl. (ISPLC'2007)*, pp. 296 – 301, March 26-28, 2007.

```

% MATLAB code for simulation;
% 15 path channel model is used;
% AWAN noise with A=0.01 and  $\Gamma=0.01$  is used;
Turbo_coded_MC-CDMA.m

clc;
clear all;
tic;
disp('Please wait simulation is going on.....!');
SNR_db=0:1:30;
T_case=length(SNR_db);
K=8; % no of users;
BER=zeros(K,T_case);
for nn=1:T_case
    no_of_iteations=4;
    err=zeros(K,no_of_iteations);
    n_err=0;
    frame_no=0;
    NL=1; % total no of frames;
    L=10000; % frame length of one user;
    SF=256; % spreading factor;
    uncoded_err=zeros(1,NL);
    SNR_NO=10^(SNR_db(nn)/10)
    rand('state',sum(100*clock));
    randn('state',sum(100*clock));

    while (frame_no)<NL
        a_data=zeros(K,L);%data of all users;
        c=zeros(K,3*L);
        %for loop is added here to fill K users Data;
        for k=1:K
            a=zeros(1,L);
            a=round(rand(1,L));%data frame;
            a_data(k,:)=a;
            z=zeros(1,L);%extrinsic information;
            b=zeros(1,L);
            b=interleaver(a);%b is the input to second encoder;
            c1=encoder(a,1);
            c2=encoder(b,2);
            %rate 1/3 turbo code.
            i=1;j=1;m=1;
            while i<=(2*L)
                while j<=L
                    c(k,m) =c1(i);
                    c(k,m+1)=c1(i+1);
                    c(k,m+2)=c2(j);
                    m=m+3;
                    i=i+2;
                    j=j+1;
                end
            end
        end
    end
end

```

```

end
c(k,:) = 2*c(k,:)-1;
end

% generating Walsh Hadmard codes for spreading;
Walsh_matrix=Walsh_hadmard(SF);
subcarriers=SF;
N=3*L; %total no of bits;
% channel
[HT H]=multipath15;
H=H(50:1585);
H=H(1:6:end);
ii=1;
r=[];

while ii<=N
    r3=[];
    spread_sum=zeros(1,SF);
    for k=1:1:K
        spread_data=c(k,ii)*Walsh_matrix(k,:);
        %summing up all the users
        spread_sum=spread_sum+spread_data;
    end
    tx=spread_sum.*H ;
    ofdm=ifft(tx,subcarriers);
    %rr=awgn(ofdm,SNR_dB(nn),'measured');
    rr=noiseA_measured(ofdm,0.01,SNR_NO);
    sigPower1 = sum(abs(ofdm(:)).^2)/length(ofdm(:));
    sigma_noise = sigPower1/SNR_NO;

    r1=fft(rr,subcarriers);
    q=(r1.*conj(H));
    r3=[];
    for k=1:1:K
        %-----combining by MRC-----;
        y=q.*Walsh_matrix(k,:);

        % -----combining by ORC-----;
        %y=q.*Walsh_matrix(k,:)/(abs(H).^2) ;

        %-----combining by EGC-----;
        %y=q.*Walsh_matrix(k,:)/(abs(H)) ;

        %-----combining by MMSEC-----;
        %y=q.*Walsh_matrix(k,:)/(K*(abs(H).^2)+sigma_noise);

        sum(y);
        s=(real(sum(y)));
        r3=cat(1,r3,s);
    end
    r=cat(2,r,r3);
    ii=ii+1;
end

reec=sign(r);

```

```

ree=0.5.*(reee+1);
cee=0.5.*(c+1);
uncoded_err(frame_no+1)=length(find(ree~=cee));

%for loop for decoding of all user data;

for ki=1:K
    rx=zeros(1,L);
    for i = 1 : L
        rx(i)=r(ki,3 * i -2);
    end
    % input to first decoder.
    input_dec1=zeros(1,2*L);
    i=1;j=1;
    while j<=(3*L-2)
        input_dec1(i)=r(ki,j);
        input_dec1(i+1)=r(ki,j+1);
        i=i+2;j=j+3;
    end
    input_dec1=input_dec1/ sigma_noise;
    limplus=find(input_dec1>125);
    input_dec1(limplus)=125;
    limminus=find(input_dec1<-125);
    input_dec1(limminus)=-125;
    %input to second decoder.
    rx2=interleaver(rx);
    input_dec2=zeros(1,2*L);
    i=1;j=1;m=1;
    while j<=L
        while m<=(3*L-2)
            input_dec2(i)=rx2(j);
            input_dec2(i+1)=r(ki,m+2);
            i=i+2;j=j+1;m=m+3;
        end
    end

    input_dec2=input_dec2/sigma_noise;
    limplus=find(input_dec2>125);
    input_dec2(limplus)=125;
    limminus=find(input_dec2<-125);
    input_dec2(limminus)=-125;

    %iterative decoding with exchange of soft information
    for nit=1 : no_of_iterations

        % calling the first decoder.
        LLR1=zeros(1,L);
        LLR1=rsc_decoder(input_dec1,z,L) ;
        LE1=zeros(1,L);
        %calculate extrinsic information (to be passed to the
        %second decoder);
        for k=1:L
            LE1(k)=LLR1(k)-(2*input_dec1(2*k-1))-z(k);
        end
        %interleave before passing to second decoder.
        extr=interleaver(LE1);

```

```

%call second decoder.
LLR2=zeros(1,L);
LLR2=rsc_decoder(input_dec2,extr,L);
LE2=zeros(1,L);
%calculate extrinsic information and interleave it.
for n=1:L
    LE2(n)=LLR2(n)-(2*input_dec2(2*n-1))-extr(n);
end
z=interleaver(LE2);
LLR=zeros(1,L);
%output log-likelihood ratio
LLR=interleaver(LLR2);
x=zeros(1,L);
%hard output after this iteration,
for i = 1:L
    if LLR(i)<0
        x(i)=0;
    else
        x(i)=1;
    end
end
%number of errors.
n_err=length(find(a_data(ki,:)-x));
err(ki,nit)=err(ki,nit)+n_err;
end
end
frame_no=frame_no+1;
end
%total BER;
for ki=1:K
    BER(ki,nn)=err(ki,no_of_iterations)/(L*NL);
end
disp('SNR = ');
disp(SNR_dB(nn));
disp('err = ');
disp(err);
end
disp('for 16 state,rate 1/3,MC CDMA, AWAN(A=0.01) results are .....')
disp('SNR in dB = ');
disp(SNR_dB);
overall_bit_error_rate=sum(err(:,no_of_iterations))/(K*L*NL);
disp('overall_bit_error_rate of coded system= ');
disp(overall_bit_error_rate);

disp('BER of uncoded MC CDMA in 3xLxK bits and NL frames');
uncoded_ber=sum(uncoded_err)/(3*L*K*NL);
disp(uncoded_ber);
toc;

%function for generation Walsh Hadmard codes;
function [Walshmatrix]=Walsh_hadmard(N)
H=1;
for i=1:ceil(log2(N))
    H = [ H H;H -H];
end;
Walshmatrix= H;

```



```

%function for generation impulse noise;
function[out]=noiseA_measured(inputvec,A,snr_no)
sigPower = sum(abs(inputvec(:)).^2)/length(inputvec(:));
sigmag = sigPower/snr_no;
%A=0.01;
T=0.01;
sigmai=sigmag*inv(T);
N=length(inputvec);
X=zeros(1,N);
Y=zeros(1,N);
Z=zeros(1,N);
out=zeros(1,N);
%randn('state',sum(100*clock));
X=randn(1,N);
for n=1:N
    a=exp(-A); b=1; i=0;
    while true
        dumml=rand;
        b=b*dumml;
        if(b<a)
            Y(n)=i;
            break;
        end
        i=i+1;
    end
    Z(n)=(sqrt((1+Y(n))*inv(T)/A)*sigmag)*X(n);
end
out=Z+inputvec;

%function for simulating Multipath channel;
function [ BB AA ]=multipath15()
k=1;
a0=0;
a1=7.8e-10;
vp=1.56e8;
g=[0.029 0.043 0.103 -0.058 -0.045 -0.040 0.038 -0.038 0.071 -0.035
    0.065 -0.055 0.042 -0.059 0.049];
d=[90 102 113 143 148 200 260 322 411 490 567 740 960 1130 1250];

Fs=4e7; % the sampling frequency 2*20MHz
f=0.01:.01:18;
f=f*1e6;
freq_points=length(f);
a= a0 + (a1*(f.^k));
di=(j*2*pi*f)/vp;
Hf=zeros(1,freq_points);
for i = 1:15
    Hf=Hf + g(i)*exp(-(a+di)*d(i));
end

hf=abs(Hf);

hdb=20*log10(hf); % frequency response
rf=f*pi/2e7;% frequency in radian
n=32;% the length of B in TF
[ B A ]=invfreqz(Hf,rf,n,n);

```

```

BB=B;
AA=A;

```

```

%function to implement the component 16-state RSC encoder;

```

```

function[out]=encoder(a,q)
L=length(a);
s=zeros(1,5);
if q==1
    for i=1:L
        s(5)=s(4);
        s(4)=s(3);
        s(3)=s(2);
        s(2)=s(1);
        s(1)=xor(a(i),xor(xor(s(2),s(3)),xor(s(4),s(5))));
        c(2*i-1)=a(i);
        c(2*i)=xor(s(1),s(5));
    end
end
if q==2
    for i=1:L
        s(5)=s(4);
        s(4)=s(3);
        s(3)=s(2);
        s(2)=s(1);
        s(1)=xor(a(i),xor(xor(s(2),s(3)),xor(s(4),s(5))));
        c(i)=xor(s(1),s(5));
    end
end
out=c;

```

```

%function to calculate the branch transition probability Gamma for a
%16-state coder;

```

```

function [G] =gamma_value(input_data1, z, i, k, md)
x=input_data1(2*k-1);
y=input_data1(2*k);
if (i==2)
    p1 = 1;
else
    p1 = -1;
end
s=zeros (1,5);
a=dec2base (md-1, 2, 5);
for d=1:5
    if a(d)==49
        s(d)=1;
    end
end
s(1)=xor(i-1,xor(xor(s(2),s(3)),xor(s(4),s(5))));
Y=xor(s(1),s(5));
p2=2*Y-1;
%Gamma value;
G=((x*p1)+(0.5*p1*z(k))+(y*p2));

```

```

%function to reverse block interleave a frame of data.
function[out]=interleaver(a)
m=length(a);
l=sqrt(m);
intl=zeros(l,l);
x=1;
for i=1:l
    for j=1:l
        intl(i,j)=a(x);
        x=x+1;
    end
end
out=zeros(l,m);
y=1;
i=1;j=1;
while j>0
    while i>0
        out(y)=intl(i,j);
        y=y+1;
        i=i-1;
    end
    j=j-1;
    i=1;
end

%function to find the last state;

function[out]=laststate(m,i)
t=zeros(2,16,16);
t(1,1,1)=1;t(2,1,9)=1;t(1,2,9)=1;t(2,2,1)=1;t(1,3,10)=1;t(2,3,2)=1;
t(1,4,2)=1;t(2,4,10)=1;t(1,5,11)=1;t(2,5,3)=1;t(1,6,3)=1;t(2,6,11)=1;
t(1,7,4)=1;t(2,7,12)=1;t(1,8,12)=1;t(2,8,4)=1;t(1,9,13)=1;t(2,9,5)=1;
t(1,10,5)=1;t(2,10,13)=1;t(1,11,6)=1;t(2,11,14)=1;t(1,12,14)=1;
t(2,12,6)=1;t(1,13,7)=1;t(2,13,15)=1;t(1,14,15)=1;t(2,14,7)=1;
t(1,15,16)=1;t(2,15,8)=1;t(1,16,8)=1;t(2,16,16)=1;

for md=1:16
    if t(i,md,m)==1
        out=md;
        return
    end
end

%function to find the next state;
function[out]=nextstate(md,i)
t=zeros(2,16,16);
t(1,1,1)=1;t(2,1,9)=1;t(1,2,9)=1;t(2,2,1)=1;t(1,3,10)=1;t(2,3,2)=1;
t(1,4,2)=1;t(2,4,10)=1;t(1,5,11)=1;t(2,5,3)=1;t(1,6,3)=1;t(2,6,11)=1;
t(1,7,4)=1;t(2,7,12)=1;t(1,8,12)=1;t(2,8,4)=1;t(1,9,13)=1;t(2,9,5)=1;
t(1,10,5)=1;t(2,10,13)=1;t(1,11,6)=1;t(2,11,14)=1;t(1,12,14)=1;
t(2,12,6)=1;t(1,13,7)=1;t(2,13,15)=1;t(1,14,15)=1;t(2,14,7)=1;
t(1,15,16)=1;t(2,15,8)=1;t(1,16,8)=1;t(2,16,16)=1;

```

```

for m = 1:16
    if t(i,md,m) ==1
        out=m;
        return
    end
end

%function to implement log-MAP algorithm
function [LLR]=rsc_decoder(input_data1,z,L)
%initializations. Trellis assumed to start with the all zero state
infinity=3e2;
A=zeros(L+1,16);
A(1,2:16)=-infinity*ones(1,15);
A(1,1)=0;
%trellis not terminated.
B=zeros(L+1,16);
B(L+1,1:16)=log(1/16)*(ones(1,16));
% forward recursion
for k1=2:L+1
    for m=1:16
        gamma=-infinity*ones(1,16);
        md=laststate(m,2);
        gamma(md)=gamma_value(input_data1,z,2,k1-1,md);
        md=laststate(m,1);
        gamma(md)=gamma_value(input_data1,z,1,k1-1,md);
        if(sum(exp(gamma + A(k1-1,:))) <=1e-100)
            A(k1,m)=-infinity;
        else
            A(k1,m) =log(sum(exp(gamma+A(k1-1,:))));
        end
    end
    %normalization to unit sum;
    for m =1:16
        if exp(A(k1,m)) ~ =0
            A(k1,m)=A(k1,m)-log(sum(exp(A(k1,:))));
        end
    end
end
%backward recursion
k=L;
while k>0
    for md=1:16
        gamma=-infinity*ones(1,16);
        m=nextstate(md,2);
        gamma(m)=gamma_value(input_data1,z,2,k,md);
        m=nextstate(md,1);
        gamma(m)=gamma_value(input_data1,z,1,k,md);
        if ((sum(exp(gamma+B(k+1,:))))<=1e-100)
            B(k,md)=-infinity;
        else
            B(k,md)=log(sum(exp(gamma+B(k+1,:))));
        end
    end
end
end

```

```

%normalization to unit sum
B(k,:) = B(k,:) - log(sum(exp(B(k,:))));
k=k-1;
end
%compute LLRs for each bit of the frame.
for k=2:L+1
    temp0=-infinity*ones(1,16);
    temp1=temp0;
    for m=1:16
        md=laststate(m,2);
        gamma1=gamma_value(input_data1,z,2,k-1,md);
        temp1(m)=exp(gamma1+A(k-1,md)+B(k,m));
        md=laststate(m,1);
        gamma0=gamma_value(input_data1,z,1,k-1,md);
        temp0(m)=exp(gamma0+A(k-1,md)+B(k,m));
    end
    if (sum(temp1)<=1e-100)
        term1=-infinity;
    else
        term1=log(sum(temp1));
    end
    if (sum(temp0)<=1e-100)
        term0=-infinity;
    else
        term0=log(sum(temp0));
    end
    LLR(k-1)=term1-term0;
end

```